NASA-CR-192407

VERY HIGH ENERGY GAMMA RAY EXTENSION OF GRO OBSERVATIONS

NASA GRANT NAG5-1381

Semiannual Status Report No. 3

For the period 1 July 1991 through 31 December 1991

Principal Investigator
Trevor C. Weekes

February 1992

Prepared for
National Aeronautics and Space Administration
Greenbelt, MD 20771

NASA GRANT NAG5-1381

1 July 1991 through 31 December 1991

Principal Investigator: Trevor C. Weekes

RESEARCH REPORT.

I. OVERVIEW

This has been an exciting year for high energy gamma-ray astronomy, both from space and from ground-based observatories. It has been a particulary active period for the Whipple Observatory gamma-ray group. In Phase I of the Compton GRO, there has not been too much opportunity for overlapping observations with EGRET and the other GRO telescopes; however significant progress was made in the development of data analsysis techniques and in improving the sensitivity of the technique which will have direct application in correlative observations in Phase II.

II. HIGHLIGHTS

(i) Completion of analysis of three year database with Whipple 10m high resolution camera.

(ii) Initial operation of new 11m telescope and first observations with stereo system.

(iii) Development of new methods of imaging analysis giving a factor of two improvement in the Crab signal detection.

(iv) Organization of workshops at Dublin ICRC and at Whipple Observatory for better cooperation in ground-based observing programs.

(v) Disemination of information on results from GRO amongst ground-based observing community.

(vi) Analysis of database for evidence of TeV gamma-ray bursts.

(vii) First upper limits of TeV emission from 3C279 presented.

III. PHYSICAL DEVELOPMENTS

(a) Focus Box.

The design for the 10 m focus box has been undertaken by our collaborators at the Ecole Polytechnique so that it can accommodate their needs in the anti-matter experiment; in particular that it will be easy to change over the 91 phototube

camera head from uv to visible with the phase of the moon. The scope of this project has been expanded to include (i) an anti-coincidence scintillator shield to provide a veto signal for local cosmic ray events and (ii) a camera head de-rotator to keep the image fixed relative to the star field. It is anticipated that this will be completed by the summer of 1992, with part of the construction being done in France and part in Tucson. We have benefitted by the design of the 11 m focus box and will incorporate many of its features into the 10 m box.

(b) Mirror Coating.

The mirror coating facility has been completed and mirrors from the 10 m reflector have been successfully stripped, re-aluminized and anodized. This hardened coating should have a ten year
lifetime. The completion of the coating facility (housed in the refurbished generator building at the Whipple Observatory) is a milestone in the development of the Cherenkov technique at the Whipple Observatory. Because of environmental concerns it was necessary to make significant modifications to the building. The aluminizing tank chamber acquired complete from government excess; it is a sophisticated device which required major work before it could be brought on-line. The mirrors from the 10 m reflector have been exposed for more than 24 years and have been recoated many times; they are now very difficult to clean and require the use of ion bombardment for a final cleansing. Thhe anodization process was not well-documented and required a certain amount of fine tuning to be satisfactory. The completed facility is highly automated so that it is easily suited to the handling of large quantities of mirrors.

Measurements of the reflectivity of the anodized mirrors show reflectivity in excess of 90% from 300 to 500 nm (the range of interest for Cherenkov work); the reflectivity of pure (non-adodized) aluminum is 92%. The measured reflectivity is also in excess of 80%down to 200 nm.

As of early January 50 mirrors have been processed i.e. removed from reflector, cleaned, aluminized, anodized, tested,

replaced and re-aligned. The remainder will be processed by the summer. It is also planned to coat glass for spare mirrors for the 11 m reflector. The addition of this facility to the Whipple gamma-ray complex is an important step towards the construction of a multi-reflector array.

(c) Computer Network.

An Ethernet Network has been completed between all the project computers on the mountain (including all PC's and the Vaxstation 3200 of the GRANITE camera). There is a similar network in the Tucson offices of the project; using the Whipple Observatory/Steward Observatory microwave link the two systems are connected together so that it is transparent to the user whether he/she is using a computer at either site. Extensive use has also been made of national/international networks to connect to computers at the other collaborating centers for the purposes of data transfer and even for running extended computing jobs.

The job of converting the 10 m mount control from Apple to PC has been completed. It is planned to use this new system for the anti-matter experiment in January, 1992.

IV. GRANITE: THE 11m REFLECTOR

Much of the local effort this year has been devoted to the physical completion and testing of the 11m reflector. In this we worked closely with the Michigan group who played the major role in the construction of the optics and electronics of the reflector. The Smithsonian group has played the prime role in the installation and testing of the mount, the installation of optics (mirrors and phototubes), the optical alignment (with ISU), the cabling, the integration of the various systems, the building, the interface between the two cameras (with MU), the testing and analysis of the first observations (with MU).

The progress on the camera installation in the calendar of progress that follows.

April,'91 : first mirror installed to coincide with launch of GRO
May, '91 : prefab building installed by contractor
June, '91 : electronics installed
July, '91 : mirrors aligned, mount control checked

August '91: focus box installed
Sept. '91 : zone 0 and 1 cables and tubes installed; first light
Oct. '91 : remaining zones installed; electronics checked
Nov. '91 : optics realigned; shower data taken
Dec. '91 : tracking completed; observations of sources
Jan. '91 : routine data taking

GRANITE is proceeding on schedule. As of December 31, 1991, the following benchmarks have been achieved:

(i) The optical point spread function has been measured to be 0.2° which is within the designed tolerance; the point spread function was measured by a star transit. Hence the optics have been made, mounted and aligned to specifications;

(ii) The tracking accuracy has been determined to be $\pm 0.1^\circ$; this is equal to the existing 10m reflector. The mount has survived several winter storms and has been reliable in operation; the mount is thus shown to be satisfactory.

(iii) The electronic camera (much of it custom-built at Michigan) has been put into operation and the recorded shower images are as predicted from our experience with the 10m camera. The parameter distributions of the background images recorded by the old 37 pixel camera on the 10m reflector and the new 37 pixel camera on the 11m reflector are comparable. The event rate is stable and is greater than 4 Hz; the electronics are thus behaving as they should. The threshold energy for gamma rays is as expected.

(iv) The outputs from the two reflectors have been interfaced and the complete stereo camera has been used to observe the Crab Nebula. Unusually bad weather has hindered observations in December so the amount of data taken is still small. In just one night of data taking on the Crab Nebula (December 31, 1991; six ON/OFF pairs) we see evidence of a signal in the individual data streams from each of the two reflectors. We are in the process of reducing the stereo data and are confident that it will indicate a significant improvement over the data taken with a single reflector. In early 1992 we will expand our observing program to observe the strong GeV sources, the unknown Geminga and the superluminal quasar, 3C279.

The bottom line then is that the two reflector system is now

in routine operation and that the first scientific results await good observing weather and detailed data analysis.

Although we are pleased with the camera performance so far, it is clear that we must proceed with the GRANITE upgrade if we are to reap the full benefit of this development. With only 37 pixels on the new camera the image resolution is inferior compared with the 10m; without modification to the 10m electronics we cannot take advantage of the inherently lower threshold and higher sensitivity of the stereoscopic system.

V. OBSERVATIONS AND DATA ANALYSIS

In June, 1991 we completed three years of observations with the high resolution camera on the 11 m reflector. In the fall we began observations in conjunction with the 11m reflector and hence entered a new era in our gamma-ray program. The International Cosmic Ray Conference in Dublin, Ireland in August, 1991 gave an opportunity for the collaboration to present a summary of these observations to the international community. Hence a special effort was made to reduce all of this three year data-base in a uniform fashion. In all a total of 19 papers (Appendix A) dealing with the Whipple project were presented at the conference by members of the collaboration; in addition the P.I. gave a plenary lecture on TeV gamma-ray astronomy (Appendix A) as well as organizing an evening workshop on calibration techniques. In this section we give a summary of the Whipple results c. December, 1991; a summary paper is now in preparation and will be submitted to the Astrophysical Journal early in 1992.

(a) Crab Nebula

The first clear detection of the Crab Nebula as a TeV gamma-ray source was reported in 1989, based on observations taken with the 37 pixel camera on the Whipple Observatory 10 m optical reflector in 1986-88 (Weekes et al. 1989). That camera was replaced in 1988 with a higher resolution 109 pixel camera (Cawley et al. 1990). Observations of the Crab Nebula with this camera over the epoch 1988-91 have been reported (Vacanti et al. 1991); here they are briefly summarized as they are the starting

point for subsequent analysis.

The 1988-89 database consisted of 65 ON/OFF pairs, comprising some 30 hours of ON source observations. The observations were taken under optimum conditions (clear sky, newly-coated mirrors, low zenith angles, etc.). The first analysis was on lines employed in the initial detection (Weekes et al. 1989) which had given a 9 sigma detection based on 60 hours of ON source observation. Candidate gamma-ray images were selected based on their orientation and shape; at the zenith this selection rejected 97% of the background. These selection criteria were determined a priori from Monte Carlo simulations of images from hadron and photon-initiated showers. The results are summarized in Table 1.

Table 1.

Azwidth-selected analysis 1988-89

Selection	Raw	Azwidth
ON	498,426	14,622
OFF	493,434	11,389
Diff.	+4,992	3,233
Sigma	+5.0	+20.0

Clearly the new camera is more sensitive than the earlier version and the reported detection is confirmed with high significance with the improved detector. The measured flux is 70 x 10^{-12}cm^{-2}s^{-1} above 0.4 TeV. Using this single parameter discriminant (Azwidth), the factor of improved flux sensitivity is 2-3.

(b) Derivation of optimum selection method: Supercuts

In the above analysis, the data (events) were calibrated and prepared for analysis essentially using the methods outlined in previous papers (Weekes et al., 1989; Vacanti et al., 1991). A more efficient method of event treatment has now been developed involving sophisticated treatments of pedestals, noise, and gains. Previously the gamma-ray selection was based principally on the Azwidth parameter using gamma domain boundaries which were predetermined by shower simulations (Hillas 1985). Here a new multi-parameter selection is described in which the domain boundaries, defined by the shape and orientation parameters, are

optimized on the data: the 1988-89 season of observations on the Crab Nebula. With this new procedure (which we call Supercuts), the significance of a source detection is increased by a factor of 1.75 (Table 2). The efficiency of the procedure is demonstrated by the application of Supercuts to new observations of the Crab Nebula in 1989-90 and 1990-91 (see below).

Since Supercuts have been optimized on this set of data the excess does not have the usual statistical significance. Below we show its application to subsequent observations of the Crab Nebula.

Table 2.

Supercuts 1988-89

	Raw	Shape	Orientation	Supercuts
ON	498,426	14,218	43,099	4,452
OFF	493,434	11,216	40,413	1,766
Diff.	+4,992	+3,002	+3,686	+2,686
Excess (sigma)	+5.0	+18.8	+12.7	+34.1

The same procedure has been used in analyzing data from several other sources (below). In these cases we can derive upper limits (or fluxes) <u>for gamma rays</u> relative to the Crab Nebula <u>provided the source spectra are similar to that of the Crab</u>; if significantly different the sensitivity may be less.

Using Supercuts, which was derived "a posteriori" from the 1988-89 Crab database, the detection level has been increased to a nominal 34 sigma. The same Supercuts selection is now applied ("a priori") to the Crab observations taken in 1989-90 and 1990-91. The results are shown in Table 3 together with the total for all three observing seasons.

Note: i) the signal is seen every year with no evidence for variability; the decline in statistical significance is consistent with the increase in energy threshold because of the decline in mirror reflectivity;

ii) the detection does not have the full significance associated with the 45.5 sigma detection since it was optimized on the first year of data;

iii) the signal is seen strongly in raw data and in selection by shape <u>or</u> orientation and shape <u>and</u> orientation;

iv) with Supercuts a signal has been isolated that is 59% gamma

rays, 41% background; the gamma-ray signal is detected at a rate of 1.2/minute and the number of gamma rays recorded from this source is 4,891;

v) in a recent paper (Akerlof et al. 1991) it is shown that the source location capability (angular resolution) of the technique for a source of this strength is a few arc-minutes (similar to EGRET);

vi) the signal is about 0.5% of the cosmic ray background; for a conventional camera which triggered on cosmic ray showers this might be about 0.2% of the background.

Table 3.

Supercut Analysis

Epoch: 1988-91 (all) Time: 4105 min Elevation: 71.3

	Raw	Shape	Orientation	Supercuts
ON	968,038	26,747	83,823	8,230
OFF	958,970	21,542	76,956	3,339
Diff.	+9,068	+5,205	+6,867	+4,891
Sigma	+6.5	+23.7	+17.1	+45.5

References.

Akerlof, C.W. et al., 1991, Ap. J. Lett., 377, L97.
Cawley, M.F. et al., 1991, Exper. Ast., 1, 173.
Hillas, A.M., 1985, 18th I.C.R.C. (La Jolla), 3, 445.
Vacanti, G. et al., 1991, Ap. J. **377**, 467.
Weekes, T.C. et al., 1989, Ap. J., 342, 379.

Center for Astrophysics
Preprint Series No. 3311

CFA CONTRIBUTIONS TO THE 22nd INTERNATIONAL COSMIC RAY CONFERENCE

Dublin, Ireland
August 11-23, 1991

Trevor C. Weekes *et al.*
Whipple Observatory
Harvard-Smithsonian Center for Astrophysics

Supercuts: an improved method of selecting gamma-rays.

M.Punch[1,2], C.W.Akerlof[3], M.F.Cawley[4], D.J.Fegan[1], R.C.Lamb[5], M.A.Lawrence[2], M.J.Lang[1], D.A.Lewis[5], D.I.Meyer[3], K.S.O'Flaherty[1], P.T.Reynolds[5], M.S.Schubnell[3].

[1] University College, Dublin
[2] Harvard-Smithsonian Center for Astrophysics
[3] University of Michigan
[4] St. Patrick's College, Maynooth
[5] Iowa State University

Introduction.

In previous reports of the detection of gamma-rays from the Crab Nebula by the Whipple Observatory imaging camera, the gamma-ray selection was based principally on the Azwidth parameter using gamma domain boundaries which were predetermined by shower simulations (1). Here we describe a new multi-parameter selection in which the domain boundaries, defined by the shape and orientation parameters, are optimized on the data: the 1988-89 season of observations on the Crab Nebula. With this new procedure (which we call Supercuts), the significance of a source detection is increased by a factor of 1.75. The efficiency of the procedure has been demonstrated by the application of Supercuts to new observations of the Crab Nebula in 1989-90 and 1990-91 (2).

Derivation of Supercuts.

Pedestals: The ADC pedestals and their RMS deviations are calculated from the data itself, which involves two passes through the data for each run.

On the first pass, the pulse height spectrum for each tube for the entire run is determined. As a first approximation, a Gaussian curve is fitted to this spectrum up to the maximum point; the pedestal and its RMS deviation taken as the center and standard deviation of this curve.

On the second pass, the pulse height spectra are calculated again, but this time omitting any tube which contains, or is adjacent to a tube which contains, a signal; a tube with a signal being defined as one which has over 4 times its RMS deviation after pedestal subtraction. The pedestal value is taken as the median of this spectrum and the RMS deviation as the standard deviation of a fitted Gaussian centered on the pedestal.

Noise: Instead of a simple global threshold (1), we define two thresholds. The picture threshold is the multiple of the RMS pedestal deviation which a tube must exceed to be part of the picture, and the boundary threshold the multiple which tubes adjacent to the picture must exceed to be part of the boundary (figure 1). The picture and boundary together make up the image; all other tubes are zeroed. Initially, the Crab 1988-89 standard database was parameterized at different values of picture and boundary threshold in order to determine their optimum values. Figures 2a,b show the variation in the signal

(number of sigma) over the picture/boundary threshold plane, which was sampled at the points shown. For the standard Azwidth cut (1), the use of a boundary does not give much improvement over the 10 dc noise threshold cut-off (1), or indeed over a cut-off based on RMS deviations in the tubes (fig. 2a).

Instead of selection on a single parameter, we now attempt to optimize the threshold selection using sets of parameters. For the initial unoptimized values for a set of cuts (Distance, Azwidth, Length, Width/Azwidth (3,8)) there is a clear 30-sigma peak at a picture threshold of 4.25 and boundary threshold of 2.25 (fig. 2b). Using the picture threshold alone (i.e., for x=y in the picture/boundary threshold plane) would give 27-28 sigma.

We have also developed noise padding procedures in software which are used to simulate the effect of padding lamps in equating the pmt noise (from night-sky light) in the ON and OFF regions. These are used only in cases of extreme brightness gradients; for most sources their use is unnecessary (for the Crab Nebula the use of software padding has no effect on the signal).

Gains: With our previous camera it had been found necessary to use gains derived from the data itself as individual pmt's had very different spectral responses; the tubes used in this new camera had a common history and it was found that the gains determined from nitrogen spark triggered test exposures were satisfactory.

Cut Values: In deciding the parameter cuts, the same database was used. It was decided to substitute a Width cut for the Azwidth cut in the set since this would allow separation of the shape and orientation elements of the cut. The results of the full set of cuts are similar using either Width or Azwidth since their values are close for images which point towards the center of the field of view.

$\cos^{-1}$(Width/Azwidth) $\sin^{-1}$(Miss/Distance) = Alpha

This parameter was suggested by the work of Aharonian et al. (8). We have chosen to define Alpha = $\sin^{-1}$ (Miss/Distance) as the interpretation is more obvious.

The dependence of the Width and Length upper cut values on size was also investigated by checking the optimum cut values when showers under various sizes were excluded. No significant change in the optimum cut value was found.

It was found that the introduction of a lower bound on the Distance cut could improve the signal. This amounts to excluding events close to the optic axis, whose orientation is not well-defined.

The optimum cut values determined are as follows:

Shape discrimination:

0.51° < Distance < 1.1°
0.073° < Width < 0.15°
0.16° < Length < 0.30°

Orientation discrimination:

0.51° < Distance < 1.1°
Miss / Distance < 0.26
(equiv. to Alpha (=$\sin^{-1}$(Miss/Distance)) < 15°)

The use of a zenith-angle dependence for the upper bound of the Width and Length cuts (of the form $w_0(\sec(z)-1)$, Hillas (3) from simulations) was investigated but was found to give no improvement in signal, so this was not used in the standard. Note that the range of zenith angle in this database was restricted to < 35°. We have however shown that the same selection works effectively on Crab data out to zenith angles of 45°.

Results

The efficacy of Supercuts can be judged from its application to the standard Crab '88/'89 database with results as follows:

	Raw	Shape	Orientation	Supercuts
ON	498,426	14,218	43,099	4,452
OFF	493,434	11,216	40,413	1,766
Diff.	+4,992	+3,002	+3,686	+2,686
Excess (sigma)	+5.0	+18.8	+12.7	+34.1

Since Supercuts have been optimized on this set of data the excess does not have the usual statistical significance. In another paper (2) we show its application to subsequent observations of the Crab Nebula. The same procedure has been used in analyzing data from several other sources. In these cases we can derive upper limits (or fluxes) for gamma rays relative to the Crab Nebula provided the source spectra are similar to that of the Crab; if significantly different the sensitivity may be less.

Conclusions.

An optimized data selection procedure has been derived based on one season of observations of the Crab Nebula; this increases the flux sensitivity by a factor of 1.75. A signal can be seen from the Crab Nebula at the > 4-sigma level in one hour of observation and a source one tenth the strength of the Crab can be detected in 30 hours. Supercuts has been applied in the analysis of a number of other sources (4,5,6). Whilst this is an improvement over the previous single parameter selection (1), it is capable of still further improvement and several parallel efforts are being made to increase the sensitivity. Alternative gamma-ray image selection methods are discussed elsewhere in the conference (8,9,10,11).

Acknowledgements.

We acknowledge the support of the U.S. Department of Energy, of NASA, of the Smithsonian Scholarly Studies Fund, and of Eolas.

References.

(1) Vacanti, G. et al., 1991, Ap. J. 377, 467.
(2) Lang, M.J. et al., 1991, this conference. OG 4.1.4.
(3) Hillas, A.M., 1985, 18th I.C.R.C. (La Jolla), 3, 445.
(4) Reynolds, P.T. et al., 1991, this conference. OG 4.5.5.
(5) Fegan, D.J. et al., 1991, this conference. OG 4.4.2.
(6) O'Flaherty, K.S. et al., 1991, this conference. OG 4.3.3.
(7) Fomin, V.P. et al., 1991, this conference. OG 10.3.4.
(8) Aharonian, F.A. et al., 1991, N.I.M., A302, 522.
(9) Reynolds, P.T., 1991, this conference. 4.7.11
(10) Hillas, A.M., West, M., 1991, this conference, 4.7.5.
(11) Pare, E, et al., 1991, this conference, OG 4.7.10.

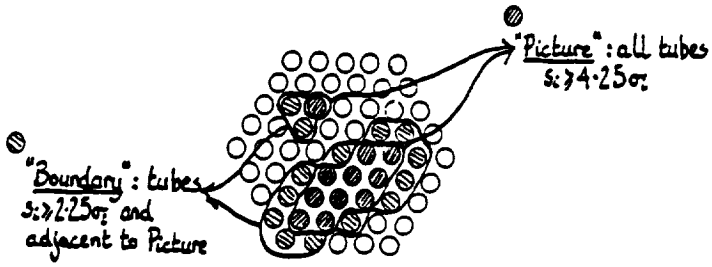

Figure 1. Definition of boundary and picture.

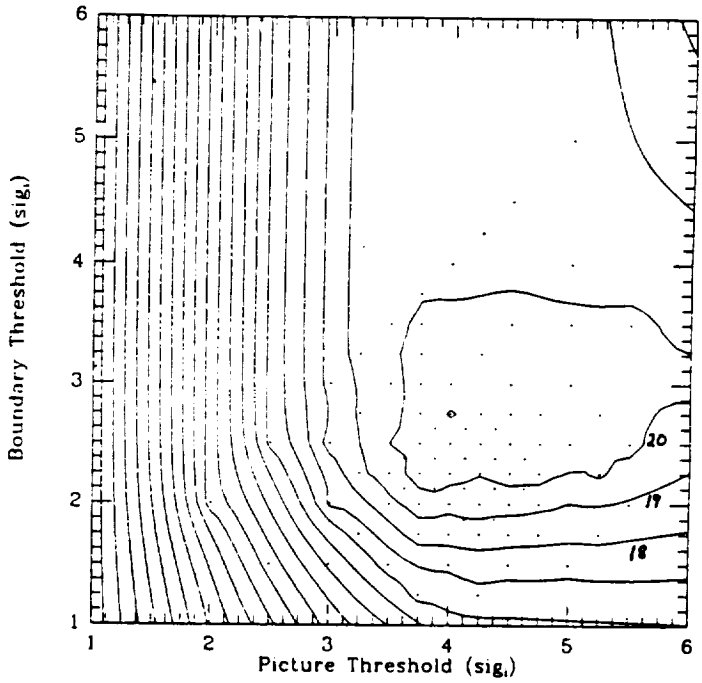

Figure 2a. Optimization of thresholds using Azwidth.

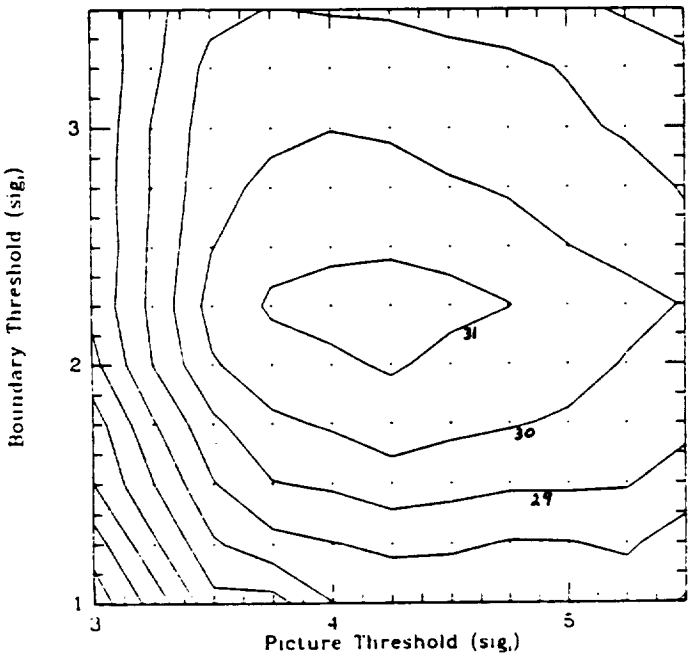

Figure 2b. Optimization of thresholds using sets of parameters.

TeV observations of the Crab Nebula and other plerions in the epoch 1988-91.

M.J.Lang[1], C.W.Akerlof[2], M.F.Cawley[3], E.Colombo[4], D.J.Fegan[1], A.M.Hillas[5], P.W.Kwok[4], R.C.Lamb[6], M.A.Lawrence[4], D.A.Lewis[6], D.Macomb[6], D.I.Meyer[2], K.S.O'Flaherty[1], M.Punch[1,4], P.T.Reynolds[6], M.S.Schubnell[2], G.Vacanti[6], T.C.Weekes[4].

1 University College, Dublin
2 University of Michigan
3 St. Patrick's College, Maynooth
4 Harvard-Smithsonian Center for Astrophysics
5 University of Leeds
6 Iowa State University

Introduction.

The first clear detection of the Crab Nebula as a TeV gamma-ray source was reported in 1989, based on observations taken with the 37 pixel camera on the Whipple Observatory 10 m optical reflector in 1986-88 (1). That camera was replaced in 1988 with a higher resolution 109 pixel camera (2); this paper reports observations of the Crab Nebula and similar objects with this camera over the epoch 1988-91.

Confirmation.

Although the initial detection was at a high level of statistical significance (9 sigma), and the signal had all the properties expected of a gamma-ray signal, the first objective of the new observing campaign was to confirm the detection with an improved detector and to demonstrate that the detector was free of systematic effects. Observations taken in the 1988-89 observing season were used for this purpose. These observations of the Crab Nebula have been reported in detail elsewhere (3).

The 1988-89 database consisted of 65 ON/OFF pairs, comprising some 30 hours of ON source observations. The observations were taken under optimum conditions (clear sky, newly-coated mirrors, low zenith angles, etc.). The first analysis was on lines employed in the initial detection (1). Candidate gamma-ray images were selected based on their orientation and shape; at the zenith this selection rejected 97% of the background. These selection criteria were determined a priori from Monte Carlo simulations of images from hadron and photon-initiated showers.

Unlike the previous report (1), a clear detection (Table 1) was apparent in the pre-selected (raw) data; this is because the hardware trigger used in this camera (two of the small (0.25 degree diameter) pixels to exceed a preset threshold) already preselects the showers of small angular dimensions expected from gamma-rays. The signal is enhanced (as predicted) using selection based on the parameters Width, Length, Miss, Conc and Azwidth. The results are summarized in Table 1 with more details given in ref.(3).

Table 1.
Azwidth-selected analysis
1988-89

Selection	Raw	Azwidth
ON	498,426	14,622
OFF	493,434	11,389
Diff.	+4,992	3,233
Sigma	+5.0	+20.0

Clearly the new camera is more sensitive than the earlier version and the reported detection is confirmed with high significance with an improved detector. The measured flux is $70 \times 10^{-12} cm^{-2} s^{-1}$ above 0.4 TeV. Using this single parameter discriminant (Azwidth), the factor of improved flux sensitivity is 2-3. The Crab detection has been independently confirmed by another experiment (4).

Azwidth-selection--1989-90 database.

In the 1989-90 observing season, the operating mode of the 109 pixel camera was changed by the addition of six 1.5 m aperture atmospheric Cherenkov telescopes to the 10 m reflector. Four of these operated in the visible, two in the ultraviolet; all had fields of view that matched that of the 10 m camera. The four visible channels, which had padding lamps, were operated as an independent trigger (at the 3 out of 4 coincidence level); their purpose was to provide an independent bias-free trigger. The camera was also self-triggered (2/91) in the absence of the independent trigger.

The mirrors were not recoated so the average threshold was somewhat higher for all showers. The independent trigger had an energy threshold about two times that of the 10 m alone and preferentially triggered on broad (non gamma-ray-like showers). Table 2 summarizes the results from all triggers as well as from independent trigger only; both unselected (raw) and azwidth-selected data are shown. It is clear that the detection is confirmed in the new data base and that the signal is statistically significant with the independent triggers (which are clearly inefficient).

Table 2.
Independent Trigger Test on Crab 1989-90.

	All Triggers		**Independent triggers**	
Selection	Raw data	Azwidth	Raw data	Azwidth
ON	282,137	9,559	125,665	930
OFF	280,249	8,252	125,607	702
Diff.	+1,888	+1,307	+58	+228
Sigma	+2.5	+9.8	+0.1	+5.6

Supercuts--1989-90.

In a companion paper (5) we report the derivation of a more sophisticated data selection routine, Supercuts, which was based on the 1988-89 Crab database. Using this "a posteriori" analysis, the detection level was increased to 34 sigma. Then the Supercuts selection was applied ("a priori") to the Crab databases taken in 1989-90 and 1990-91. The results are shown in Table 3 together with the

total for all three observing seasons.

We note: i) the signal is seen every year with no evidence for variability; the decline in statistical significance is consistent with the increase in energy threshold; ii) the detection does not have the full significance associated with the 45.5 sigma detection since it was optimized on the first year of data; iii) the signal is seen strongly in raw data and in selection by shape or orientation and shape and orientation; iv) with Supercuts we have isolated a signal that is 59% gamma rays, 41% background; the gamma-ray signal is detected at a rate of 1.2/minute and the number of gamma rays recorded from this source is 4,891; v) in a companion paper (6) we show that the source location capability (angular resolution) of the technique for a source of this strength is a few arc-minutes (similar to EGRET); vi) the signal is about 0.5% of the cosmic ray background; for a conventional camera which triggered on cosmic ray showers this might be about 0.2% of the background.

Table 3.
Supercut Analysis

Epoch: 1988-89	Time: 1808		Elevation:	69.8
	Raw	Shape	Orientation	Supercuts
ON	498,426	14,218	44,099	4,452
OFF	493,434	11,216	40,413	1,766
Diff.	+4,992	+3,002	+3,686	+2,686
Sigma	+5.0	+18.8	+12.7	+34.1
Rate(av)/min	272.9			

Epoch: 1989-90	Time: 1232 min		Elevation:	72.0
	Raw	Shape	Orientation	Supercuts
ON	282,137	7,331	23,635	2,290
OFF	280,249	5,832	21,688	904
Diff.	+1,888	+1,499	+1,947	+1,386
Sigma	+2.5	+13.1	+9.1	+24.5
Rate(av)/min	227.5			

Epoch: 1990-91	Time: 1065 min		Elevation:	73.0
	Raw	Shape	Orientation	Supercuts
ON	187,475	5,198	16,089	1,488
OFF	185,287	4,494	14,855	669
Diff.	+2,188	+704	+1,234	+819
Sigma	+3.6	+7.1	+7.0	+17.6
Rate(av)/min	174.0			

Epoch: 1988-91 (all)	Time: 4105 min		Elevation:	71.3
	Raw	Shape	Orientation	Supercuts
ON	968,038	26,747	83,823	8,230
OFF	958,970	21,542	76,956	3,339
Diff.	+9,068	+5,205	+6,867	+4,891
Sigma	+6.5	+23.7	+17.1	+45.5

Variability.

The average run duration was 28 minutes; the distribution of the excesses per run, after the application of Supercuts, was examined. We find no evidence for

variability on this timescale.

A search has also been made for evidence of periodic emission at the pulsar period. The data-base for this analysis was expanded from that used above since it was possible to include tracking observations under non-optimum conditions. The expanded database covered 7,390 minutes. The resulting light curve for the three years of Supercuts data folded at the Crab period using the pulsar ephemeris (7) is shown in Figure 1. As reported previously we find no evidence for direct pulsar emission (1,3).

We have also searched for short-term periodic emission on a run-by-run basis. Of the 250 runs examined in the expanded database, we find only one run to be statistically somewhat anomalous. This occurred on January 11, 1991 starting at U.T. 04.02 and lasting for 29 minutes. It shows a Crab-like light-curve with probability (allowing for the number of runs tested) < 1% of being a random fluctuation. It was a tracking run but was bracketed by other runs which did not show any evidence for periodic emission.

Other Plerions.

We have expanded our observing program to include observations on two other plerions (supernova remnants with centrally-filled morphologies); at first sight none of these could be expected to have the intensity of the Crab Nebula. The results of these observations are given in Table 4.

Table 4.
Plerions.

Source	Time. (min.)	Supercuts ON	OFF	Excess	Energy (TeV)	Flux < $x10^{-12}cm^{-2}s^{-1}$
3C58	403	484	446	+38 (+1.2)	0.55	32
SS433	191	280	279	+1 (+0.0)	0.55	18
PSR0656	84	191	200	-9 (-0.5)	1.0	34

Acknowledgements.

We acknowledge the assistance of Kevin Harris and Teresa Lappin in making the observations. We also acknowledge the support of the U.S.D.O.E., NASA, the Smithsonian Scholarly Studies Fund and Eolas, the Irish scientific funding agency.

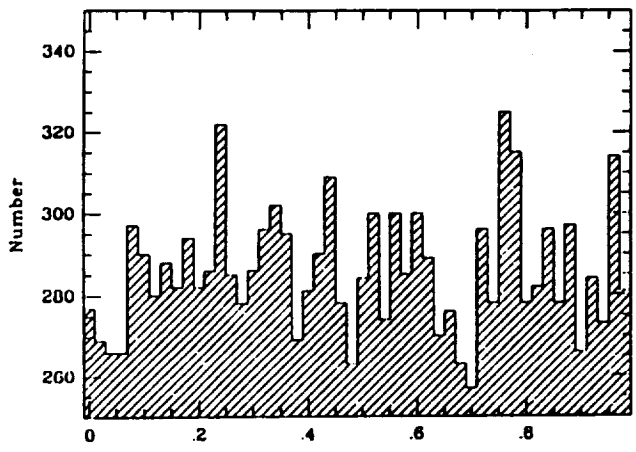

Figure 1. Light-curve of PSR0531 (Supercuts).

References.

(1) Weekes, T.C. et al., 1989, Ap. J., 342, 379.

(2) Cawley, M.F. et al., 1991, Exper. Ast., 1, 173.

(3) Vacanti, G. et al., 1991, Ap. J., 377, 467.

(4) Akerlof, C.W. et al.,1990, 21st ICRC(Adelaide), 2,135.

(5) Punch. M. et al., 1991, this conference, OG 4.7.3.

(6) Akerlof, C.W. et al., 1991, this conference, OG 10.3.1.

(7) Lyne, A.G, Pritchard, R.S.,1991, private communication.

Search for TeV Gamma-ray Emission from Classical Gamma-ray Sources with the Whipple Imaging Telescope.

C.W.Akerlof[1], M.F.Cawley[2], M.Chantell[3], D.J.Fegan[4], R.C.Lamb[5], M.A.Lawrence[3], M.J.Lang[4], D.A.Lewis[5], D.I.Meyer[1], G.Mohanti[5], K.S.O'Flaherty[4], M.Punch[4], P.T.Reynolds[5], M.S.Schubnell[1], T.C.Weekes[3], T.Whitaker[3].

1 University of Michigan
2 St. Patrick's College, Maynooth
3 Harvard-Smithsonian Center for Astrophysics
4 University College, Dublin
5 Iowa State University

Introduction.

Much of the excitement in VHE gamma-ray astronomy has come from the observation of the episodic periodic galactic sources. This has led to the relative neglect of a wide spectrum of "classical" sources. These are characterized by the fact that emission of TeV gamma rays is expected at some level, based on theoretical predictions or on observations at longer wavelengths. The predicted level is uncertain and may be below the level achievable with the present generation of detectors; here we report observations on these sources with the Whipple telescope.

Method.

The Whipple Observatory imaging telescope and the observing method are described elsewhere (1); the gamma-ray selection method is outlined in a companion paper (2) and its effectiveness demonstrated on observations of the Crab Nebula (3). All observations were made between May, 1988 and June, 1991. Energy threshold and flux limits are quoted assuming an energy spectrum similar to that of the Crab Nebula. All upper limits are at the three sigma level and, as usual, a factor of 1.5 uncertainty is assigned to the absolute value of energy threshold and collection area.

Observations: Extended Sources.

Diffuse Background: there are no detailed theoretical predictions of the diffuse background at TeV energies but, by extrapolation, it is expected to be about 10^{-5} of the cosmic ray background at comparable energies. The atmospheric Cherenkov imaging technique offers the first possibility to measure the flux because of the ability to discriminate gamma-ray showers from those caused by hadrons. Because the flux is diffuse, only the shape parameter, Width, can be used. Simulations show that a range of Width from 0.04° to 0.12° includes 71% of the diffuse gamma-ray component. Based on 5 hours of observation at the zenith the percentage of detected events in this range is determined (3.8%); a high fraction of these events come from local cosmic rays passing through the phototubes. This fraction was measured (with camera closed) and found to be 2.96% of the total. The percentage of true cosmic ray shower events within the gamma-ray

domain is then 0.84±0.13%. Allowing for the triggering inefficiency of background showers compared to gamma-ray showers and the collection area for gamma rays, we estimate an upper limit (>0.4 TeV) $I_{gamma}/I_{hadron} < 1.1x10^{-3}$.

Galactic Plane: two six hour drift-scans across the plane gave an upper limit of $1.9x10^{-9} cm^{-2}s^{-1}rad^{-1}$ with energy 0.4 TeV for a source region ±5° of galactic latitude using shape selection only; this agrees with limits reported previously for E > 0.9 TeV (4).

Giant Molecular Clouds: there have been several predictions of VHE emission from G.M.C.'s. Because of their large extent they are not ideally suited for observation with narrow beam atmospheric Cherenkov telescopes. Here we report the first upper limit on the Taurus GMC as $< 1.8x10^{-11} cm^{-2}s^{-1}$ above 0.5 TeV where gamma-ray event selection has been limited to shape (Width) only. The energy spectrum is plotted in Figure 1a.

Observations: Discrete Sources.

In Table 1 we report the results of observations on a variety of classical discrete sources.

Table 1.
Observation Summary

	Raw	Shape	Orientation	Combined
2CG135	Epoch: Oct-Nov,'90			
ON	22,976	791	2,022	130
OFF	22,854	782	1,995	118
Diff.	+122	+9	+27	+12
Sigma	+0.57	+0.23	+0.43	+0.76
GeV-A	Epoch: May,1990			
ON	45,143	1,150	3,827	193
OFF	44,986	1,122	3,723	184
Diff.	+157	+28	+104	+14
Sigma	+0.5	+0.5	+1.2	+0.7
3C273	Epoch: 1989,1991.			
ON	320,093	10,869	41,389	1,674
OFF	319,659	10,794	40,963	1,580
Diff.	+434	+75	+426	+94
Sigma	+0.5	+0.5	+1.5	+1.6
3C279	Epoch: 1989.			
ON	110,969	6,552	10,528	975
OFF	111,728	6,443	10,549	1,001
Diff.	-759	+109	-21	-26
Sigma	-1.6	+1.0	-0.1	-0.6
NGC4151	Epoch: 1990-91			
ON	201,063	2,417	15,211	439
OFF	200,812	2,455	15,187	387
Diff.	+251	-38	+24	+52
Sigma	+0.4	-0.5	+0.1	+1.8
M87	Epoch: 1989			
ON	194,713	4,386	15,997	688
OFF	194,869	4,424	15,927	634
Diff.	-156	-38	+70	+54
Sigma	-0.2	-0.4	+0.4	+1.5

Some of these results are discussed below:

2CG135+1 (MeV/GeV source): this was first reported as a gamma-ray source by the SAS-2 experiment. Our upper limit (Table 2) is based on the assumption that the source is at the center of the error circle and has a Crab-like spectrum.

Geminga (Mev/Gev source): this much studied object was a high priority object for observations. A large database was accumulated but gave somewhat inconclusive results. Further observations with an improved telescope (4) should resolve the issue. An upper limit of less than 20% of the flux of the Crab can be quoted with confidence.

GeV-A (GeV source): the Japanese aircraft experiment (6) reported the apparent detection of a number of sources with energies > 40 GeV. The strongest of these, A, was observed in May, 1990 with null results. Because of positional uncertainty, the upper limit quoted in Table 2 has been based on shape discrimination only. The energy spectrum is shown in Figure 1b.

3C273 (MeV/GeV source,quasar): previously reported upper limits (6) are updated (Table 2 and Figure 1c).

3C279(Mev/GeV source, quasar): this is reported as a new variable source in May 1991 by Egret on GRO. Observations reported previously (7) are reanalyzed with Supercuts (2) and a new upper limit reported in Table 2 and Figure 1d.

NGC4151(MeV source, AGN): observations taken in 1990-91 at high elevation give a strong upper limit (Table 2).

M87 (radio-galaxy): this strong radio galaxy with conspicuous jet has been predicted to be a source of TeV gamma rays; no evidence for gamma-ray emission is found in these observations (Table 2).

SN1990B,1991T (extragalactic supernova): these two relatively bright supernova were observed soon after initial outburst; there is no evidence for emission. The latter source was later observed by GRO.

Table 2.
Upper Limits.

Source	Class	Time. (min.)	Elevation (deg.)	Energy (TeV)	Flux $<10^{-12}cm^{-2}s^{-1}$
2CG135	MeV/GeV	140	59	0.55	16
GeV-A	GeV	214	61	0.45	32
3C273	AGN/GeV	1,586	54	0.48	5.1
3C279	AGN/GeV	453	46	0.40	14
NGC4151	AGN/MeV	1,132	74	0.50	3.6
M87	Radiogal.	745	65	0.40	7.0
SN1990B	Supernova	223	66	0.45	11
SN1991T	Supernova	111	59	0.55	14

Conclusion.

Although the Whipple imaging camera, with Supercuts, offers a significant improvement over previous telescope sensitivities no emission is found from a wide variety of predicted sources. Some of these may be detectable with the next generation of detectors (4).

Acknowledgements.

We acknowledge the assistance of Kevin Harris and Teresa Lappin in making the observations. We also acknowledge the support of the U.S.D.O.E., NASA, the Smithsonian Scholarly Studies Fund and Eolas, the Irish scientific funding agency.

References.

(1) Cawley, M.F. et al. 1991, A. and A., 243, 143.
(2) Punch, M. et al., this conference, OG 4.7.3
(3) Lang, M.J, et al., this conference, OG 4.1.4
(4) Reynolds, P.T. et al., 1990, 21st ICRC, **2**, 383.
(5) Akerlof, C.W. et al., this conference, OG 10.3.1
(6) Enomoto, R. et al., 1990, Phys. Rev. Lettr. 64, 2063.
(7) Vacanti, G. et al., 1990, 21st ICRC, Adelaide, 2, 329.

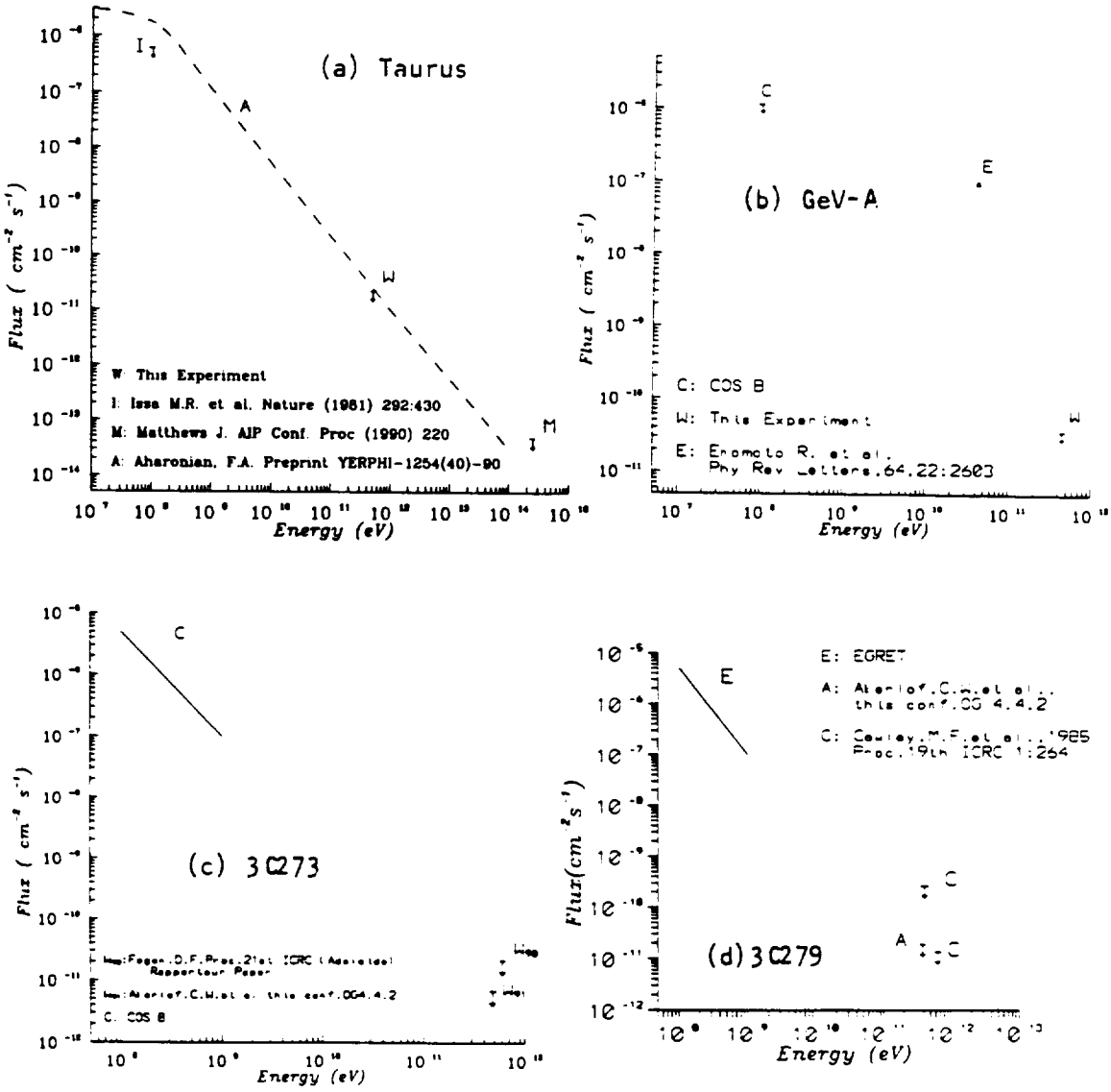

Figure 1. Energy spectrum of (a) Taurus GMC; (b) GeV A; (c) 3C273; (d) 3C279.

A Search for TeV Gamma-ray Emission from Binaries and Pulsars with the Whipple Imaging Telescope.

P.T.Reynolds[1], C.W.Akerlof[2], M.F.Cawley[3], M.Chantell[4], E.Colombo[4], D.J.Fegan[5], J.Hagan[5], M.A.Lawrence[4], M.J.Lang[5], D.A.Lewis[1], D.Macomb[1], D.I.Meyer[2], G.Mohanty[1], S.Murphy[5], K.S.O'Flaherty[5], M.Punch[5], M.S.Schubnell[2], T.Whitaker[4].

[1] Iowa State University
[2] University of Michigan
[3] St. Patrick's College, Maynooth
[4] Harvard-Smithsonian Center for Astrophysics
[5] University College, Dublin

Introduction.

TeV emission has been reported from many x-ray binaries, radio pulsars and cataclysmic variables. In almost all cases the reported signal is periodic and episodic with the episodes lasting from minutes to days. In most cases the signals reported did not have the properties expected of gamma-ray showers. We have used the Whipple Observatory high resolution imaging telescope to observe a selection of these objects; detailed reports on some of these sources have been reported elsewhere. (1,2,3,4).

Method.

The Whipple Observatory imaging telescope and the observing method are described elsewhere (5); the gamma-ray selection method is outlined in a companion paper (6) and its effectiveness demonstrated on observations of the Crab Nebula (4,7). Observations were in two forms: ON/OFF as used for steady sources and tracking (ON only) when weather conditions were less than optimum. The latter were used to supplement the database in searching for periodicity. All observations were made between May, 1988 and June, 1991. Energy threshold and flux limits are quoted assuming an energy spectrum similar to that of the Crab Nebula. All upper limits are at the three sigma level and a factor of 1.5 uncertainty is assigned to the absolute value of energy threshold and collection area.

Results.

The sources are listed in Table 1 together with details of the analysis using Supercuts (7). No statistically significant signals were seen from any of the sources, either in terms of a net excess or a steady or episodic periodic signal. Upper limits for the net excess are quoted in Table 2 for the sources observed; in the absence of definite predictions it is difficult to quote meaningful upper limits from the periodic searches. For the radio pulsars our limits are based on an assumed 10% duty-cycle with all observations phase-linked.

Table 1.
Source Summary.

	Raw	Shape	Orientation	Supercuts
Her X-1	Epoch: 1988-91			
ON	284,397	3,256	25,056	523
OFF	282,976	3,387	24,852	542
Diff.	+1,421	-131	-204	-19
Sigma	+1.89	-1.6	+0.9	-0.6
V0332+53	Epoch: 1988			
ON	88,569	3,254	7,531	575
OFF	89,033	3,433	7,417	549
Diff.	-464	+179	+114	+26
Sigma	-1.1	-2.1	+0.9	+0.8
SCO X-1	Epoch: 1990			
ON	108,442	9,361	10,493	1,497
OFF	108,406	9,326	10,602	1,453
Diff.	-36	+35	-109	+44
Sigma	+0.1	+0.3	-0.7	+0.8
4U2129+47	Epoch: 1990			
ON	56,145	2,113	4,889	332
OFF	55,684	2,041	4,742	316
Diff.	+461	+72	+147	+16
Sigma	+1.4	+1.1	+1.5	+0.6
1E2259+58	Epoch: 1990			
ON	59,242	2,478	4,889	377
OFF	58,692	2,355	4,934	378
Diff.	+554	+123	-45	-1
Sigma	+1.6	+1.8	-0.4	-0.0
Am Her	Epoch: 1990-91			
ON	120,020	2,508	9,778	423
OFF	119,968	2,587	9,820	410
Diff.	+52	-79	-42	+13
Sigma	+0.1	-1.1	-0.3	+0.4
PSR0950	Epoch: 1988-91			
ON	137,497	2,585	10,985	416
OFF	137,154	2,551	11,148	419
Diff.	+343	+34	-163	-3
Sigma	+0.6	+0.5	-1.1	-0.1
PSR0355	Epoch: 1988-91			
ON	455,934	10,201	37,548	1,572
OFF	456,386	10,487	37,049	1,650
Diff.	-452	-286	+499	-78
Sigma	-0.5	-2.0	+1.8	-1.4
PSR1855+09	Epoch: 1988-91			
ON	47,231	1,372	3,931	187
OFF	47,919	1,476	4,009	223
Diff.	-688	-104	-78	-36
Sigma	-2.2	-1.9	-0.8	-1.8

We discuss some of the sources below:

Her X-1 (binary): This is one of the best observed and best established binary sources with all reports based on the observation of episodic outbursts of periodic emission. A summary of six years of observations of this source by the Whipple telescope has been published elsewhere (3). In this report the database has been extended by another year

of observations with the high resolution camera; again no significant emission is detected. An upper limit to the steady emission is found at a level 1/20th that of the Crab Nebula.

4U0115+63 (binary): No new observations or analyses are reported here; a summary paper has been published elsewhere (1).

4U2129+47 (binary): This binary was suggested as a potential TeV emitter by K.S.Cheng (private communication); no net excess or periodicity is found in 1990-91. Because of a brightness gradient in the vicinity of this source (and of the source which follows below) it was necessary to add padding lamps in software to make noise in the ON and OFF regions consistent.

1E2259+58 (binary): This was reported by the Durham group at the Adelaide ICRC as a possible source. Upper limits based on observations by the Whipple group have been published elsewhere (2); the data reported here is taken in 1990-91 and again no periodicity is found in the expanded database which included an extra 350 min. An upper limit to the periodic gamma-ray signal (sine wave) was derived from 300 minutes of data which was phase-linked over 14 days, similar to that in the original discovery; this limit was $< 14 \times 10^{-12} cm^{-2} s^{-1}$ (fig. 1).

Am Her (Cat.var.): Gamma-ray emission has been reported from several cataclysmic variables including this one; observations in 1990-91 showed no evidence for TeV emission.

PSR0950 (radio pulsar): This was one of the first pulsars discovered and is one of the closest; no evidence for periodic emission is found in the expanded database (with an extra 917 min). The upper limit to steady periodic emission with a 10% duty cycle is $< 0.34 \times 10^{-12} cm^{-2} s^{-1}$.

PSR0355 (radio pulsar): This is an unusual pulsar in that large glitches in the radio period have been reported. TeV emission was reported by the Tata group after a large glitch; no subsequent emission has been seen. There was a total of 2,328 minutes of tracking data used in the periodicity analysis. An upper limit to steady periodic emission with a 10% duty cycle is $1.3 \times 10^{-12} cm^{-2} s^{-1}$.

PSR1855+09 (msec pulsar): This 5.4 msec pulsar is nearby and has been suggested as a source by K.Bretcher. Emission has been reported by the Durham group. Our database for periodicity analysis gives a limit of $< 1.8 \times 10^{-12} cm^{-2} s^{-1}$.

Acknowledgements.

We acknowledge the assistance of Kevin Harris and Teresa Lappin in making the observations. We also acknowledge the support of the U.S.D.O.E., NASA, the Smithsonian Scholarly Studies Fund and Eolas, the Irish scientific funding agency.

Table 2.

Upper Limits to steady emission (ON/OFF).

Source	Class	Time. (min.)	Elevation (deg.)	Energy (TeV)	Flux < $10^{-12}cm^{-2}s^{-1}$
Her X-1	Binary	1404	72	0.48	3.3
V0332+53	Binary	352	64	0.40	12
Sco X-1	Binary	635	40	0.75	12
4U2129+47	Binary	336	63	0.55	11
1E2259+58	Binary	362	65	0.55	11
Am Her	Cat. Var.	748	63	0.55	5.5
PSR0950	Radio pulsar	499	63	0.40	8.3
PSR0355	Radio pulsar	2,032	62	0.45	4.0
PSR1855	msec pulsar	305	58	0.60	9.5

References.
(1) Macomb, D. et al., 1991, Ap. J., 376, 738.
(2) Cawley, M.F. et al., 1991, A. and A. 243, 143.
(3) Reynolds, P.T. et al., 1991, Ap. J., (in press).
(4) Lang, M.J. et al. 1991, this conference, OG 4.1.4.
(5) Cawley, M.F. et al., 1991, Exper. Ast. 1, 173.
(6) Punch. M. et al., 1991, this conference, OG 4.7.3.
(7) Vacanti, G. et al., 1991, Ap. J., 377, 467.

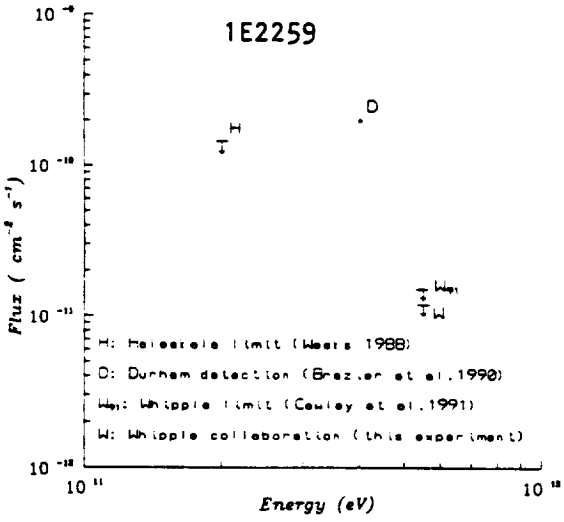

Figure 1. Energy spectrum of 1E2259+58

OG.4.3.3

Upper Limits to the TeV emission from Cygnus X-3 in 1988-90

O'Flaherty,K.S.[1], Cawley,M.F.[2], Fegan,D.J.[1], Lang,M.J.[1], Lewis,D.A.[3], Punch,M[1,4], Weekes,T.C.[4].

1 Physics Department, University College, Dublin, Ireland.
2 Physics Department, St. Patrick's College, Maynooth, Ireland.
3 Physics Department, Iowa State University, Ames, U.S.A.
4 Harvard-Smithsonian Center for Astrophysics, U.S.A.

Introduction:

The low mass X-ray binary system Cygnus X-3 has been the subject of intense study at all wavelengths. In the energy range 0.1 to 10 TeV it has been observed to be a highly variable emitter of γ-rays (1) while in the PeV energy range there have been reports of possible γ-ray detections . Recent reports summarised in (1) suggest that it may also be a source of EeV γ-rays (2,3), although this is disputed in (4). The objective of the Cygnus X-3 observations during 1988-'90 was to acquire data with a view to looking at both raw and γ-ray data for steady emission, 4.8 hour modulation of the γ-ray light curve and periodic emission at 12.59 ms.

Observations:

Observations on Cygnus X-3 were made using the Whipple Observatory high resolution imaging camera (5). The camera head consists of 91 pixels (each with a field of view of 0.25°), surrounded by an outer ring of 18 pixels (each with a field of view of 0.5°), giving a full field of 3.75° diameter. The camera is triggered by the coincidence of signals from a preset number of photomultiplier tubes each exceeding a threshold of 40 photoelectrons. For the observations reported here the trigger requirement was a 10 nanosecond coincidence between any 2 of the inner 19 photomultiplier tubes. This gives an effective energy threshold of 0.4 TeV. For each shower the digitized image of the Čerenkov light pattern in the camera was recorded as well as its time of arrival.

Analysis and Results:

The 1988 to 1990 Cygnus X-3 database consists of 49 hours of ON/OFF data, taken under excellent sky conditions. Data reduction methodology followed closely the procedure adopted for analysing the Crab Nebula database (6,7); briefly, this involved subjecting each data file to flat-fielding and calibration prior to the application of shower image parameterization (ie:the "SUPERCUTS" procedure). This parameterization selects γ-ray candidates on the basis of their shape and orientation in the camera's focal plane. With this procedure we are confident that we can reject up to 99.6% of the hadronic background from our data, resulting in a small, but γ-ray rich, candidate database.

Both the raw and γ-ray databases were analysed for evidence of steady emission of TeV γ-rays, the characteristic 4.8 hour orbital periodicity and 12.59 ms pulsar periodicity.

(a) Steady emission of TeV γ-rays.

For both the raw and γ-ray events, the scan by scan totals of events observed both ON and OFF source (N_{on} and N_{off}) were accumulated. For each scan pair, the ON/OFF ratios and significances S (in standard deviations σ) were calculated using the expression of Li and Ma (8).Statistics on the yearly totals were also accumulated and these are summarized in Table 1.

Table 1
Summary of Results

Year	Raw Data N (pairs)	Raw Data N (on)	Raw Data N (off)	Raw Data Effect (S)	γ-ray Data N (on)	γ-ray Data N (off)	γ-ray Data Effect (S)	Elevation (average)
1988	6	59194	59333	-0.4	350	352	-0.1	64°
1989	42	363382	364522	-1.3	1555	1584	-0.5	68°
1990	32	229230	229483	-0.4	643	664	-0.6	70°
Total	80	651806	653338	-1.3	2548	2600	-0.7	

Table 1: ON source and OFF source statistics for raw and γ-ray data.

It is clear from the entries in Table 1 that there is no evidence for any steady flux of γ-rays from Cygnus X-3 for the 1988 to 1990 database. The distributions of the significances of the raw and γ-ray data on the basis of individual scans are consistent with random expectation, the most extreme values being -3.3σ for a raw pair in 1989 and $+2.9\sigma$ for a raw pair in 1990. There is no evidence for any steady flux of γ-rays from Cygnus X-3 for the observational intervals in question or for any statistically significant individual scans. The 3σ upper limit for the γ-ray data is 3.5×10^{-12} photons cm^{-2} s^{-1}. For the raw data the corresponding value is is 3.9×10^{-11} photons $cm^{-2}s^{-1}$. These upper limits are presented along with recent upper limits from other experiments in Fig. 1. Also shown is the spectrum derived from earlier observations (9).

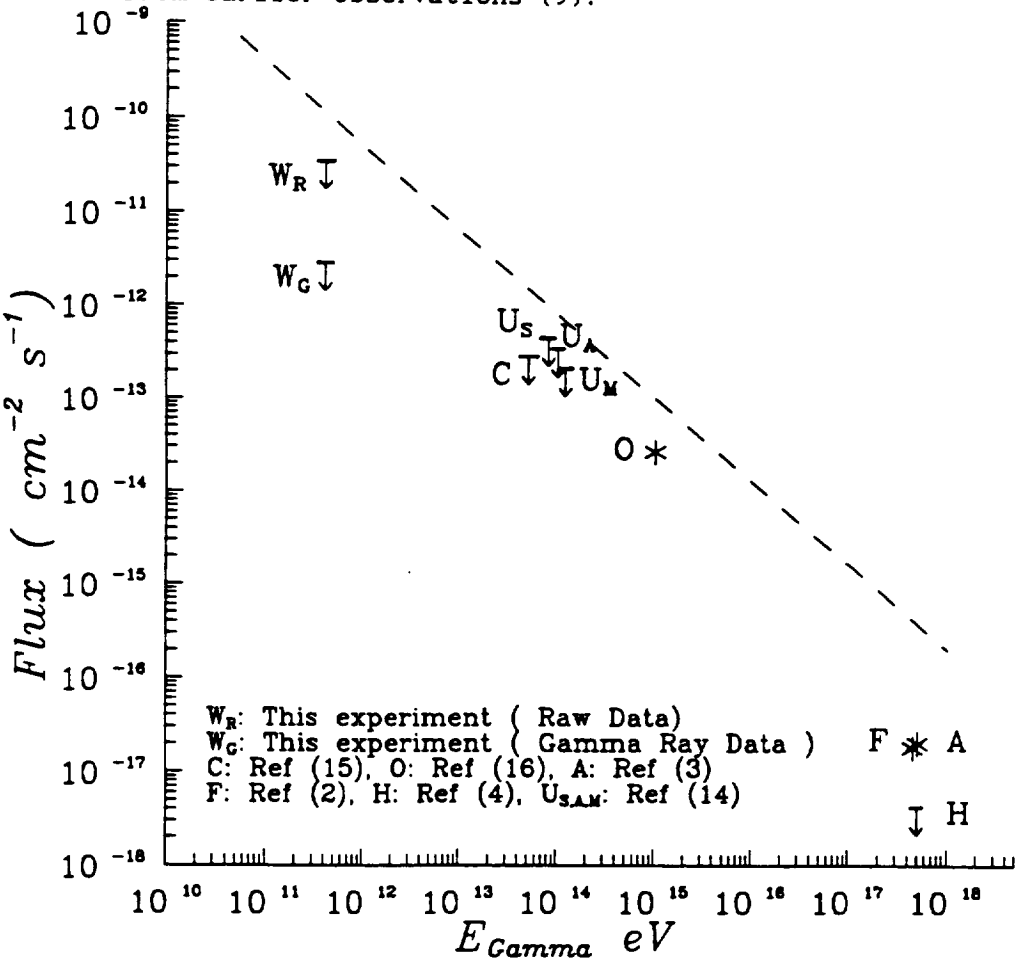

Figure 1: Recent upper limits on the flux from Cygnus X-3.

(b) 4.8 hour Binary Orbit Period Modulation.

The Whipple Observatory database has been examined for possible evidence of 4.8 hour modulation. Since the orbital period is close to one fifth of a day, this has the consequence that scan pairs taken during the course of any dark period will tend to be phase locked with the local sidereal time. This in turn leads to somewhat incomplete coverage of the 4.8 hour cycle. For the purpose of observing the distribution of events as a function of the 4.8 hour phase we have used the quadratic ephemeris of van der Klis and Bonnet-Bidaud (10). The full 4.8 hour period has been divided into 12 phase intervals of 24 minutes duration. The resultant light curves for both the raw and γ-ray data are featureless with no significant peaks in any of the phase bins. This negative result is in agreement with most of the contemporaneous observations on the 4.8 hour modulation at TeV and PeV energies (1).

(c) Periodic emission of γ-rays at 12.59 ms.

Repeated attempts by the Whipple collaboration (1,11) to confirm the reports of a 12.59 ms pulsar in the Cygnus X-3 system (1,8) have been unsuccessful. These attempts were always very specific in that they attempted to test the Durham hypothesis, that the periodic emission is linked to a very specific point in the orbital motion of Cygnus X-3. Other groups have also failed to confirm the Durham observations . However, the Adelaide group have recently claimed new evidence for the 12.6 ms pulsar using the low elevation Čerenkov technique (12). They have shown that a particular 10 minute segment of 5 nights of combined data for August - September 1989 shows the occurence of significant periodicity at 12.5953 ± 0.0002 ms (probability for combined nights is $\cong 7 \times 10^{-7}$), at an orbital phase of 0.564 (exactly which ephemeris was used was not specified). The Durham group would have predicted a phase of 0.62 with a pulsar period of 12.5962 ± 0.0004 ms. Based on the Adelaide findings, the Durham group examined their September 1989 database and found evidence (13) in a 300 second segment of data taken on September 7th of periodic emission with a period of $\cong$ 12.5953 ms, at a probability level of $\cong 10^{-8}$. For the purpose of analysing the 1988-'90 Whipple data, we have calculated the phase using the quadratic polynomial of the new van der Klis and Bonnet-Bidaud X-ray ephemeris (ephemeris III).

To test the hypothesis, the 1988-1990 database was examined for scans which spanned the 0.56 phase range based upon ephemeris III. A total of twenty-four scans satisified this criterion. The relative times of arrival of events in these scans (recorded to a precision of 1μs with an absolute accuracy of 0.5ms) were corrected to the barycentre using the JPL-DE200 ephemeris. For each scan, those events which lay within the phase range 0.54 to 0.63 were extracted for periodic analysis. Each scan which satisified this criterion was analysed by moving a 300 second window through the data in steps of 60 seconds. In order to test for possible continuous low-level periodic emission, rather than just large periodic power outbursts, we have examined the entire power spectrum in the following manner. Corrected event times were analysed using a Rayleigh analysis over the target period range corresponding to 20 independent trial periods (with an oversampling factor of 5) between 12.59 ms to 12.60 ms. A parent distribution was generated over the 1000 independent trial periods between 12.33 ms and 12.87 ms (excluding the 20 periods of the target range). Each scan was subjected to this form of periodic analysis and the normalised power levels were combined and binned for both the target and parent distributions. The analysis of the γ-ray data was in two parts: (1) data selected by a shape cut; (2) data selected by an orientation cut. Neither of these analysis showed any evidence for statistically significant periodicity. The combination of the two cuts (Supercuts) on average left only 7 events per five minute interval and hence was not suitable for Rayleigh analysis.The resultant differential power

spectra are shown in Fig. 2. Using the Anderson and Darling test (17) ,we estimate the probability that the parent and target values are drawn from the same distribution to be 99% for each of the three data sets. We would therefore conclude that there is no evidence in this database for a periodic γ-ray signal pulsed at 12.59 ms.

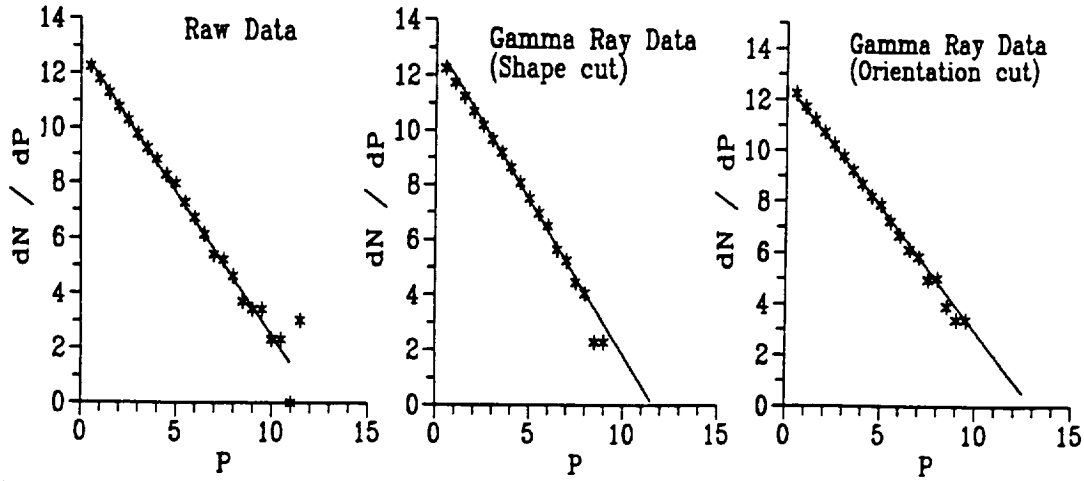

Figure 2: Differential power spectra for Raw data and γ-ray data. (* = target values, — = background values)

Conclusions.

We have observed Cygnus X-3 for a total of 49 hours during the combined 1988 to 1990 observing seasons. We find no evidence for any long term steady emission of TeV γ-rays and estimate 3σ upper limits of 3.5×10^{-12} photons $cm^{-2}s^{-1}$ for the raw data. For the γ-ray data analysis this limit is 3.9×10^{-11} photons $cm^{-2}s^{-1}$. We see no evidence for any 4.8 hour periodicity, with featureless light curves in both the raw data and γ-ray data sets. These conclusions are in broad agreement with most of the TeV and PeV observations of Cygnus X-3 pertinent to the observations taken during the latter half of the nineteen-eighties. The results of our search for evidence of a 12.59 ms periodicity in the 1988 to 1990 Cygnus X-3 database continues to yield null results, consistent with our previous analysis of the 1983 to 1986 database.

Acknowledgements: We acknowledge the assistance of Kevin Harris and Teresa Lappin in making the observations. We also acknowledge the support of the U.S.D.O.E, NASA, the Smithsonian Scholarly Studies Fund and EOLAS, the Irish scientific funding agency.

References.

(1) Fegan, D.J. 1990, Proc. 21st I.C.R.C. (Adelaide) 11,23
(2) Cassiday,G.L. et al, 1989, Phys. Rev. Lett. 62, 383
(3) Teshima, M. et al, 1990 Phys. Rev. Lett. 64, 1628
(4) Lawrence, M.A. et al, 1989, Phys. Rev. Lett. 63, 11, 1121
(5) Cawley,M.F., et al, 1990, Exp. Astron. 1, 173
(6) Punch,M. et al, 1991, This conference.
(7) Lang,M.J. et al,1991, This conference.
(8) Li, Ti-pei and Ma, Yu-qian, 1983, Astrophys. J. 272, 317,324
(9) Weekes, T.C.
(10) van der Klis,M. and Bonnet-Bidaud,J.M., 1989, Astron. Astrophys.,214,203
(11) O'Flaherty,K.S., et al, 1990, Proc. 21st I.C.R.C.(Adelaide) 2,2
(12) Brazier,K.T.S, et al, 1990, Astrophys.J. 350,745
(13) Bowden, C.C.G. et al, 1990, AIP Conf. Proceedings 220,75
(14) Krimm, H.A. et al, 1990, AIP Conf. Proceedings 220,122
(15) Alexandreas, D.E. et al, 1990, Phys. Rev. Lett. 64,2973
(16) Muraki, Y. et al, 1991, Astrophys. J. 373,657
(17) Anderson, T.W and Darling, D.A. 1952, Annals of Math. Stat. V23,193

A Search for TeV Bursts of Gamma-rays.

V. Connaughton[1], M.Chantell[2], D.J.Fegan[1], N.A.Porter[1], T.C.Weekes[2].

[1] University College, Dublin
[2] Harvard-Smithsonian Center for Astrophysics

Introduction.

The Whipple Observatory Imaging Gamma-ray Telescope (1) is uniquely suited to a search for gamma-ray bursts at TeV energies for a number of reasons. These include: a) low energy threshold; b) large field of view and hence large collection area; c) discrimination against hadronic showers and hence good flux sensitivity; d) high angular resolution within the field of view; e) good energy resolution. Equally important is that the detector has been used to detect a flux of gamma-rays from the Crab Nebula and hence its properties have been proven and are well-understood (2). The results of a search for primordial black holes (pbh) with this instrument have been reported previously (3); here we refine the technique and extend this search to look for pbh's as well as classical gamma-ray bursts.

(a) Search for Primordial Black Holes

Searches have been made for primordial black holes through their explosive evaporation into gamma-ray bursts (3,5). Generally results have been ambiguous or negative, yielding only upper limits to the pbh density. Two nuclear models have been considered; here we present data that is relevant only to the elementary particle model (3) in which 10^{30} ergs of gamma rays at 5 TeV are produced in the burst within 0.1 seconds. In a recent paper (6) in which the phenomenon is reviewed these numbers are reevaluated; in particular the threshold energy is raised to 10 TeV.

The present work is similar to search (B) in the Adelaide paper (3) and again used the Whipple 10 m reflector with 109 tubes (field of view 3.5°); however the observations were made at a zenith angle of 75°, giving a greatly increased collection area (10^{10} cm^2) and increasing the threshold energy to 10 TeV. Because the large zenith angles were beyond the range of normal operation of the 10 m gamma ray observing program, the exposure was limited to 10 hours of dedicated operation under clear skies. Observations made with the phototubes covered indicated that 80% of the events triggering the camera at this zenith angle are due to local secondary cosmic rays passing through the phototubes. This increases the background but does not introduce systematic burst-like effects.

The event rate was 0.78 Hz. The usual procedures were used for treating the raw data and selecting candidate gamma-ray events. In this case, because of the large zenith angle the selection was somewhat different and was based on the parameters, Width and Frac3. Frac3 is defined as the ratio of the sum of the three highest pixels to the sum of all pixels. Unfortunately no simulations of the Cherenkov images expected from gamma rays at these large zenith angles were available; the gamma-ray domain was chosen by extrapolation of simulations at smaller angles. Demanding Width $< 0.15^{\circ}$ and Frac3 < 1.0 gave a database that was 30% of the total raw database (70% rejection). These shape-selected events were then the basis for the search for bursts with three events in a 0.1 sec time interval; two candidate bursts were found. This occurrence rate is consistent with random expectation. If the gamma rays were from a cosmic burst then they should have a common point of origin; this implies that a further selection can be made on the basis of orientation with the point of origin anywhere within the camera field of view. Figure 1a shows the first "burst" in which there is clearly no point of intersection. Figure 1b shows the second "burst" in which, given the uncertainty in axes determination (about 15°), the three axes could intersect (although the displacement from the centroid makes a common origin unlikely).

Although we do not regard this event as a plausible detection we calculate an upper limit for the current rate of pbh explosions based on the detection of one event in 10 hours. This observed rate is compatible with an upper limit (Poisson probability at the 90 % level) to the mean rate of two events within the observing interval.

The solid angle of the system, O, is about 3.0×10^{-3}. The collection area is $10^{10} cm^2$. The energy required for a burst is 24 ergs (3 gamma rays). Thus the minimum flux sensitivity, S $= 2.4 \times 10^{-9}$ erg-cm^{-2}.

If r is the maximum distance for detection, then

$$4 \pi r^2 = 8 \times 10^{30} / 2.4 \times 10^{-9}$$
$$r^2 = 2.65 \times 10^{38}$$
$$r = 1.6 \times 10^{19} = 5.4 \text{ pc}$$

The volume of space covered, $V = O r^3 / 3 = 0.16$ pc^3.
The time of observation, $T = 3.7 \times 10^4$ sec $= 1.2 \times 10^{-3}$ yrs.
Then the upper limit is $2/(1.2 \times 10^{-3} \times 0.16) = 10^4$ pc^3-yr.

In conclusion we find no convincing evidence for gamma-ray bursts consisting of three events with threshold energy of 10 TeV within 0.1 sec; the upper limit derived is slightly below that of previous experiments (1). Improved sensitivity will come from i) reduction of the background cosmic ray rate using a two-fold coincidence (9); ii) Monte Carlo simulations of gamma-ray showers at high zenith angles; iii) increased exposure time.

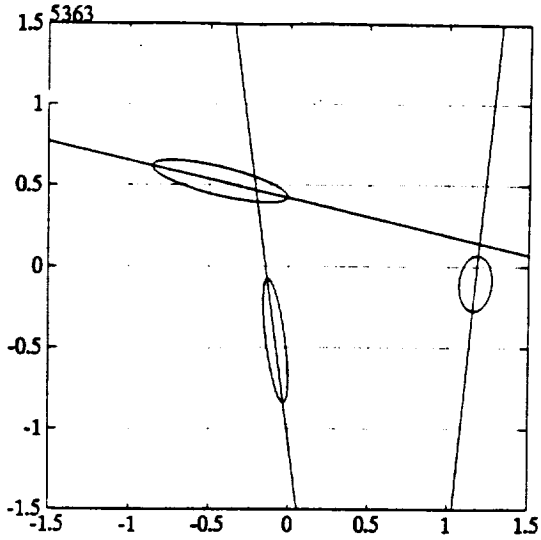

Figure 1a. Candidate burst that is rejected.

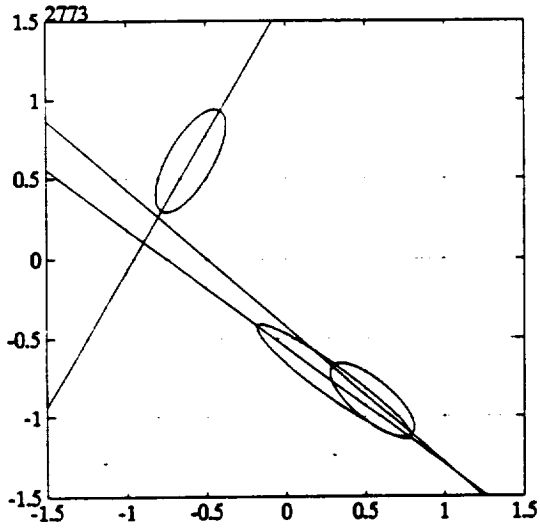

Figure 1b. Candidate burst that is almost acceptable.

(b) **Classical Gamma-ray Burst Search.**

Although most gamma-ray burst searches at TeV energies have concentrated on the verification of the important pbh phenomenon, it has been pointed out (K.S.Cheng, private communication) that conventional gamma-ray bursts (at 1 to 100 Mev energies) may have a high energy gamma-ray counterpart. Cheng et al. (7) have compared the measured gamma-ray spectra with those predicted by their outer gap model and find reasonable agreement. The outer gap model also predicts almost equal gamma-ray luminosity at MeV and at TeV energies (8). A typical gamma-ray burst of 10^{-6} erg cm^{-2} s^{-1} would result in about 600 detectable gamma-rays in

the field of view of the 10 m reflector and thus would be easily detectable on time-scales of seconds; however the rate of such events would be only a few per year of running time. In practice assuming a reasonable spectrum of burst energies, bursts of 10 gamma-rays might occur at a rate of one per 300 hours of operating time (K.S.Cheng, private communication).

The search for bursts on these longer time-scales is very similar to the PBH search. As before initially a selection is made based on the shower image parameters to select only candidate gamma rays. For this purpose a selection was made based on a combination of the parameters, Width and Length, the optimum values being determined from the simulations of gamma-ray showers. The values used were Width $< 0.15^{\circ}$ and Length $< 0.30^{\circ}$; with this selection 93% of the events recorded are rejected as being of hadronic origin. The efficiency for gamma-ray detection is estimated at 70%. The database used consisted of 102.5 hours of data taken in the direction of the sources the Crab Nebula, Hercules X-1, 4U0115+63, Cygnus X-3, V03332, PSR0950, and 3C273, and their comparison areas, all at elevation $> 50^{\circ}$. After the above selection a search was made for bursts of 1 and 10 second duration. With a threshold of 5 (11) events for a burst on a 1 (10) s timescale we found 60(328) potential bursts.

In a true burst the events would come from a common point in the camera field of view. Each potential burst was tested accordingly using a "Roving Miss" cut in which the camera was divided into a grid of 40 by 40 points which were tested as potential points of origin for the burst. With an average trigger rate of 200 per minute we would expect, after software selection, 0.23 background events in 1 s and 2.3 events in 10 s. In a burst the other (5 - 0.23) and (11 - 2.4) events would come from a single point within the grid. In practice we found two bursts in which there were 4 or more (1 s) and two with 8 or more (10 s) events from a common grid point (Miss $< 0.14^{\circ}$. These are consistent with random expectation; based on this we derive an upper limit to the TeV gamma-ray burst rate of 0.07 hr^{-1} (assuming an energy threshold of 0.4 eV). This does not seriously constrain the outer gap model of gamma-ray bursts. A more significant limit may arise if a burst detected by GRO occurs within the field of view of the camera during simultaneous observations of particular source directions.

References.

(1) Cawley, M.F., et al., 1991, Exper. Ast., 1, 173.
(2) Vacanti, G. et al., 1991, Ap. J., 377, 467.
(3) Nolan, K. et al., 1990, 21st ICRC (Adelaide), 2, 150.
(4) Page, D.M., Hawking,S.W., 1976, 206, 1.
(5) Porter, N.A., Weekes, T.C., 1978, M.N.R.A.S., 183, 202.
(6) Halzen, F. et al., 1991, Nature, (in press).
(7) Cheng, K.S. et al., 1986, Ap. J., 300, 500 and 522.
(8) Cheng, K.S., de Jager, O.C., 1990, in press.
(9) Akerlof, C.W., et al., 1991, this conf., OG 10.3.1

Comparison of the Imaging Gamma-ray Telescopes at the Crimean and Whipple Observatories.

V.P.Fomin[1] , K.S.O'Flaherty[2,3], A.P.Kornienko[1], Yu.I.Neshpor[1], P.T.Reynolds[4], V.G.Shitov[1], A.A.Stepanian[1], B.M.Vladimirsky[1], T.C.Weekes[3], Yu.L.Zyskin[1].

[1] Crimean Astrophysical Observatory
[2] University College, Dublin
[3] Harvard-Smithsonian Center for Astrophysics
[4] Iowa State University

Atmospheric Cherenkov telescopes are being developed in several countries at present which record the image of the detected air showers in Cherenkov light (1,2,3). The camera in these cases is an array of photomultipliers in the focal plane whose analog outputs are recorded digitally on command. A schematic view of the cameras of the Crimean Astrophysical Observatory (1) and the Whipple Observatory (2,3) is shown in Figures 1a,b,c. In all of the cameras the photomultipliers are arranged in hexagonal patterns. The characteristics of the cameras are summarized in Table 1.

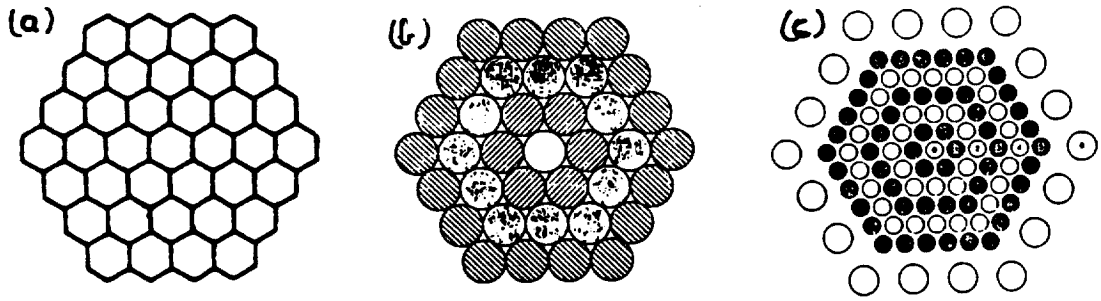

Figure 1. View of the focal plane (a) for the Crimean camera (b) for the Whipple Medium Resolution and (c) for the Whipple High Resolution cameras.

Using these cameras it is possible to characterize the images of the showers in terms of parameters such as image size and orientation. These parameters are then used to select events as candidate gamma-rays. If this selection is to be effective, then the parameters should be as true as possible to those obtained with a perfect camera i.e. free of all distortions. Since each pixel consists of a separate photomultiplier, amplifier and analog-to-digital converter, it is necessary to accurately determine the relative gain of each channel. This process is the equivalent of flat-fielding in astronomical cameras. It is essential that the illumination of the flat-field be as similar as possible to that of the air shower light image; this is not trivial to achieve since the light pulse is short and has a broad spectral range. At the Crimean Observatory the calibration light source used was a low power nitrogen laser; at the Whipple Observatory the calibration light source was a nitrogen spark gap.

Table 1.
Camera Characteristics.

	Crimea	Whipple	
		Medium	High
No. of Pixels	37	37	109
Pixel spacing (deg)	0.38	0.5	0.25
Full field diameter, (deg.)	2.6	3.75	3.5
Light Cones	Yes	No	No
Energy Threshold(TeV)	2.0	0.4	0.3

Gain calibrations are never perfect and it is often difficult to assess how successful they are. The Crimean group has recently described a method for determining the quality of the flat-fielding (4). The basic idea was that the quality of the flat-field could be assessed from the distribution of the position angles of the elliptical images; the position angle is defined as the angle the major axis of the image makes with the horizontal axis through the center of the field of view. The modulation (RMS) of this distribution as a function of angle is a measure of the uniformity of the camera. This distribution is shown in Figure 2a for the Crimean camera and in Figure 2b,c for the Whipple Medium and High Resolution cameras (labelled "before"); in each case the gains have been applied based on the calibration light flashes. The modulation is seen to be

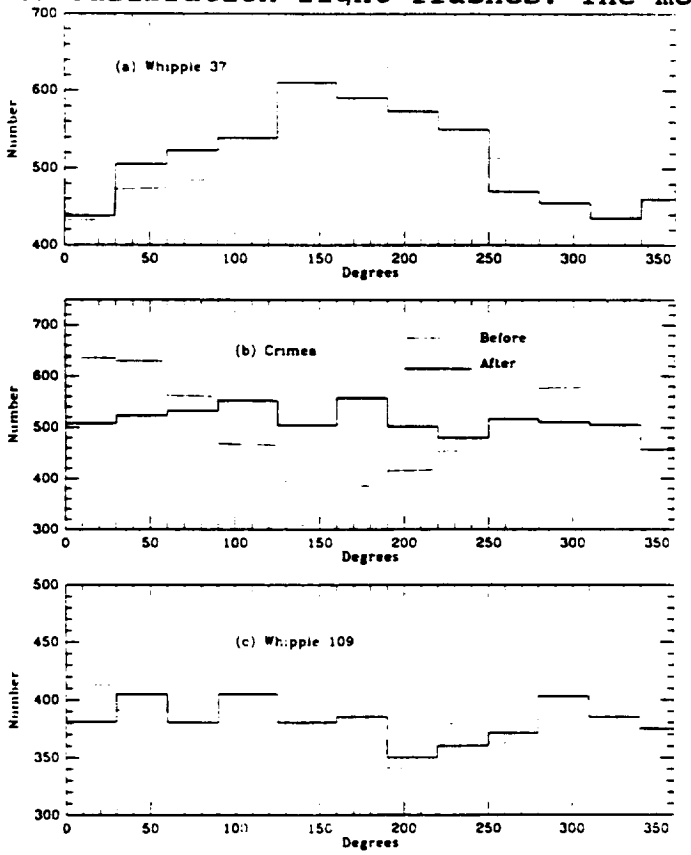

Figure 2. Distribution of the position angle of the Cerenkov images for (a) Whipple Medium (b) Crimean (c) Whipple High both before and after the final gain calibration.

of order 15% in each case but for the Whipple High Resolution camera the modulation is only 5%. There are several reasons why the modulation should still remain after the calibration (e.g. the difference in triggering thresholds in each pixel, uneven spectral response, etc.,) but special investigations are necessary to determine the cause in each case.

It is possible reduce the modulation using additional gain calibrations. Each of the two groups came to the conclusion that this could be achieved using the measured spectra of light pulse amplitudes of air showers in each channel. These spectra are shown in Figure 3 a,b for the Crimean and Whipple 37 element cameras where the spectra have been averaged over the respective zones (hexagonal rings). In each case the spectra of the non-edge zones show a region where the spectrum can be described by a power law with integral spectral index = -1.5. This corresponds to the spectrum of the underlying cosmic rays. One can assume that the spectra of individual channels should show this spectral index and that the gains should be adjusted to make this true. This provides a second stage of gain calibration; note the calibration can only be carried out within zones and the light pulse must be used for calibration between the zones. Failure to achieve uniformity after this procedure may be caused by the relative triggering efficiency of neighboring channels.

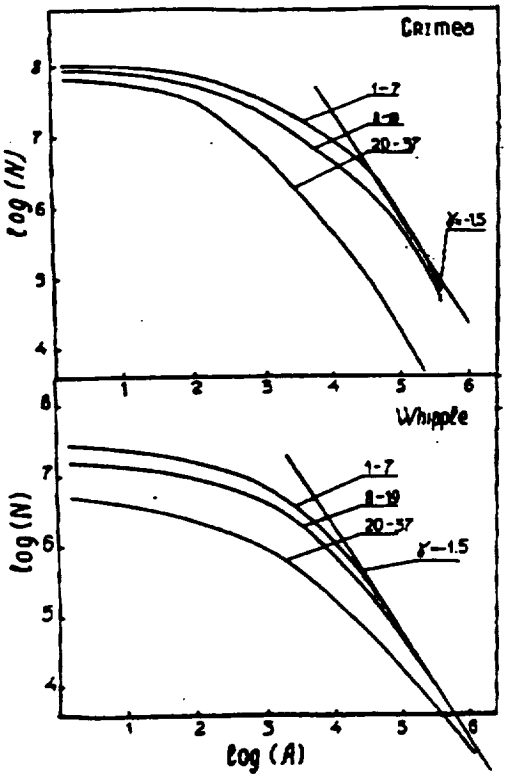

Figure 3. The spectra of the light flashes amplitudes for the two 37 pixel cameras averaged over the respective zones.

The distribution of the position angles after this procedure (Figure 2a,b,c "after") shows that the modulation is reduced to about 5% for the Crimean camera but for the Whipple Medium Resolution camera it makes little improvement. For the Whipple High Resolution camera the modulation is reduced to 3%.

It is useful also to compare the distribution of image parameters as determined by the two 37 pixel cameras. Figure 4 shows the distribution of the parameters Length, Width and Concentration for the two 37 pixel cameras. The Length and Width distributions are very similar. Small differences can be caused by the difference in pixel sizes, the energy thresholds, and the elevation of the observatories. The largest differences are seen in the Concentration distributions which for the Crimean camera are smaller than the Whipple camera which is consistent with the larger pixel size in the latter.

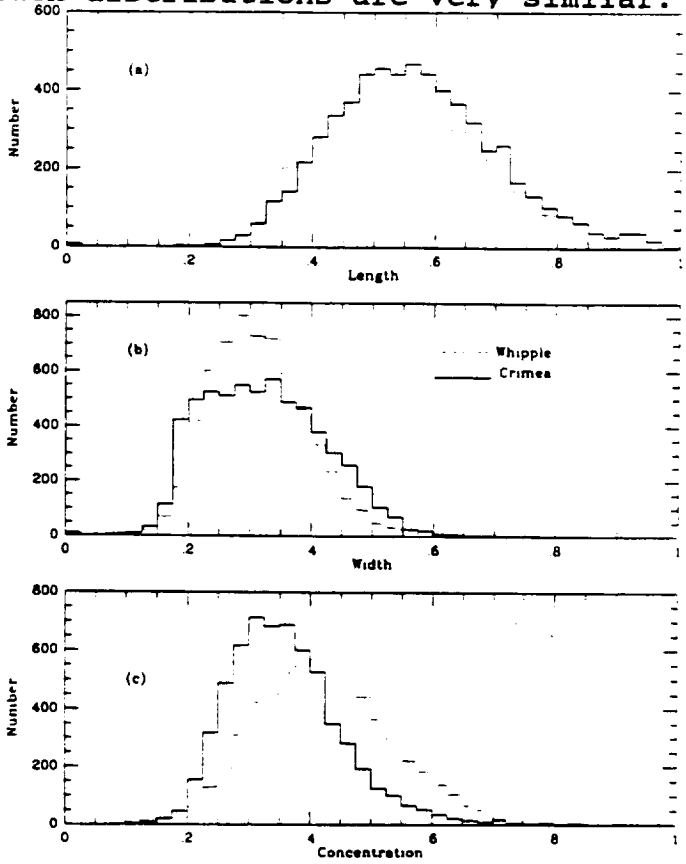

Figure 4. Distributions of measured values of "length", "width" and "conc" for the two 37 pixel cameras.

In conclusion we emphasize that these two independent cameras give similar results which indicates that the atmospheric Cherenkov technique is well understood and can be applied to the study of gamma-rays with confidence. The question of the optimum size and number of pixels is still open and requires further investigation.

Acknowledgements.

This work was supported in part by the U.S. Dept. of Energy and the Smithsonian Scholarly Studies Fund. VPF acknowledges the hospitality of the Smithsonian Institution where this work was completed.

References.

1. Vladimirsky et al., 1989, Proc. of Internat. Workshop on VHE Gamma Ray Astronomy, Crimea, USSR, April, 1989, p.21.
2. Weekes et al., 1989, Astrophys. J., 342, 379.
3. Cawley et al., 1991, Exper. Astron., 1, 173.
4. Vladimirsky et al., 1991, Izv. Krimskoi Astrophys. Obs. (in press).

Locating Very High Energy Gamma-ray Sources with Arc Minute Accuracy.

C.W.Akerlof[1], M.F.Cawley[2], M.Chantell[3], D.J.Fegan[4], K.Harris[3], A.M.Hillas[5], D.G.Jennings[6], R.C.Lamb[6], M.A.Lawrence[3], M.J.Lang[4], D.A.Lewis[6], D.I.Meyer[1], G.Mohanty[6], K.S.O'Flaherty[4], M.Punch[4], P.T.Reynolds[6], M.S.Schubnell[1], T.C.Weekes[3], T.Whitaker[3].

1 University of Michigan
2 St. Patrick's College, Maynooth
3 Harvard-Smithsonian Center for Astrophysics
4 University College, Dublin
5 University of Leeds
6 Iowa State University

Introduction.

Recently, ground-based experiments have demonstrated the ability to unambiguously detect TeV gamma-rays from the Crab Nebula (Weekes et al. 1989). The Cherenkov air shower technique, using a tenuous radiator (air), detects an electromagnetic shower cascade several kilometers long and a few tens of meters wide. The characteristic narrow transverse dimensions of these showers permits rejection of the far greater background flux of hadronically initiated events. By selecting air showers based on the predicted characteristics of Cherenkov light images, a 20 sigma detection of the Crab at gamma-ray energies above 400 GeV has proven the efficacy of this technique (Weekes et al. 1989, Vacanti et al. 1991).

The image selection reduces the hadronic background for two independent reasons. First of all, the hadronic showers are broader in width because the typical interaction imparts a transverse momentum of the order of a pion mass to the secondary particles. The comparative transverse momentum for electromagnetic showers is set by the electron mass which is 270 times smaller. Secondly, hadronic shower directions are isotropic since the trajectory of the parent charged particle is thoroughly randomized by the intervening galactic magnetic fields. Thus, a selection based on the apparent arrival direction of the shower considerably favors gamma-rays from a compact source relative to the hadronic background.

Roughly speaking, Cherenkov light images of electromagnetic showers can be characterized as elongated ellipses with the major axis representing the projection of the shower trajectory on the image plane. The location of the source must lie along this axis near the tip of the light distribution corresponding to the initial interaction of the shower cascade. With a single imaging telescope, one shower image alone cannot pinpoint the source direction but many events can be combined to restrict the common phase space to a relatively small area of the sky. The characteristic ratio of shower Width to Length implies that the shower direction can be measured to a precision of the order of 0.2°. By averaging over N events, the source location error can be reduced by $1/N^{1/2}$, at least until systematic errors begin to dominate. We have carried through this type of analysis for two sets of

observations of the Crab Nebula, one with the telescope pointing directly at the known sky position and the other with the telescope tracking a fixed point shifted in declination by 0.4° above the Crab. The number of events associated with the Crab signal was significantly larger than 100 for both measurements so that systematic tracking errors are more significant than the statistical errors. In each case, we find that the source location reconstructed from the shower images agrees with the tracking location to approximately 2 arc minutes. At this level, the dominant error can be attributed to the telescope angle encoders and the drive system which have 5 arc minute tolerances.

Method.

The technique can best be understood in terms of the schematic diagram of the Whipple 10-meter telescope high resolution camera shown in figure 1 (a detailed description of this apparatus can be found in Cawley et al. 1990). Three different geometric structures are depicted in overlapping layers. The 109-tube photomultiplier array of the high resolution camera is shown at the lowest level. The camera consists of an inner cluster of 91 29 mm diameter tubes surrounded by an outer ring of 18 51 mm diameter tubes. The second overlapping structure is a Cartesian grid system covering an interval of $\pm 1.0°$ in both right ascension and declination directions. Each mesh point will be treated as a possible gamma-ray source direction in the sky. Finally, a hatched ellipsoid depicts the outline of a typical shower image and three associated image parameters. Note that the image WIDTH and LENGTH are independent of the source position but the so-called AZWIDTH parameter depends sensitively on this assumed location. In figure 1, the indicated AZWIDTH value corresponds to a source direction at the center of the Cartesian grid. In general, each of the 441 mesh points will be associated with a different value. The procedure is to consider every mesh point as a possible source location. For each event, the image parameters are checked for compatibility with the gamma-ray selection criteria previously developed. Those mesh points far from the true source direction will tend to have large values of AZWIDTH and so few events will be consistent with gamma-rays emanating from a point source from these parts of the sky. Conversely, for mesh points near the source direction, most true gamma-ray events will be accepted. By carrying out this process for every shower in the data sample, a three dimensional histogram can be constructed of events versus right ascension and declination within a field of view of $\pm 1.0°$. The results are shown in figure 2 for data taken on the Crab Nebula during 1988-1989. The total exposure was approximately 60 hours, divided equally between on-source and off-source observations. In figure 2a, the number of showers is plotted for data accumulated with the telescope pointed directly at the Crab Nebula and figure 2b shows data taken off-source with the telescope pointed several degrees away. Clearly, the on-source data is qualitatively different in shape. The broad central maximum apparent in the off-source data is an artifact of the event selection criteria

used to reduce the hadronic background. Figure 2c shows a plot of the difference signal. The statistical significance of the signal is greater than 20 sigma. As can be seen from the figure, the signal is an approximately Gaussian function of right ascension and declination with a circular probable error of 0.23° (14 arc minutes). The center of the distribution can be determined to a small fraction of this value.

To prove this last point, a much shorter data exposure (4 hours on-source, 4 hours off-source) was taken with the gamma-ray telescope tracking a celestial coordinate deliberately offset by a fixed angle from the Crab Nebula (0.4° in declination). The results are shown in figure 3. A contour plot of the on-source minus off-source distribution shows an 8 sigma peak displaced from the origin. The center of the peak was determined by interpolation and compared with the known tracking offset. The values agreed to an accuracy of 0.036° or 2 arc minutes. At this level of precision, the telescope tracking error will predominate so for future data taking, a CCD camera has been coaxially mounted to record the true sky position by simultaneous direct optical measurement of several nearby field stars. The Crab Nebula was also observed for a total of 22 hours (half on-source, half off-source) with a 1.0° offset to the tracking direction. At this limit of the telescope field of view, the efficiency for detecting gamma-rays was noticeably diminished.

A more complete description of this technique as well as an alternative method of deriving the angular resolution has been published elsewhere (Akerlof et al. 1991b).

These analyses show that Cherenkov air shower imaging techniques are sensitive over a moderately large field of view with spatial accuracies considerably better than any other available gamma-ray detector at any energy. For comparison, the COS-B collaboration quoted a circular probable error of 0.4° (24 arc minutes) for the location of Geminga. Figure 4 shows a map of radio and X-ray sources that lie within this boundary. The expected error circles for EGRET and the Whipple twin gamma-ray telescope system are also plotted. The arc minute resolution of ground-based observations would almost certainly provide a unique identification of Geminga with the radio and X-ray counterparts.

If the sensitivity of the new generation of VHE detectors (Akerlof et al. 1991a) can reach the flux levels required, ground-based experiments may provide considerable help in identifying the specific sources responsible for energetic gamma-ray emission.

Acknowledgements.

This work was supported, in part, by the U. S. Department of Energy, the Smithsonian Scholarly Studies Fund, and Eolas, the Irish Scientific Funding Agency.

REFERENCES

Akerlof, C. W., *et al*. 1991a, this conference, 10.3.1.
Akerlof, C.W., *et al*.. 1991b, Ap. J. Lettr. (in press).
Cawley, M. F., *et al*. 1990, *Experimental Astronomy* 1, p. 173.
Vacanti, G. *et al*. 1991, Ap. J., (to be published).
Weekes, T. C. *et al*. 1989, Ap. J. **342**, p. 379.

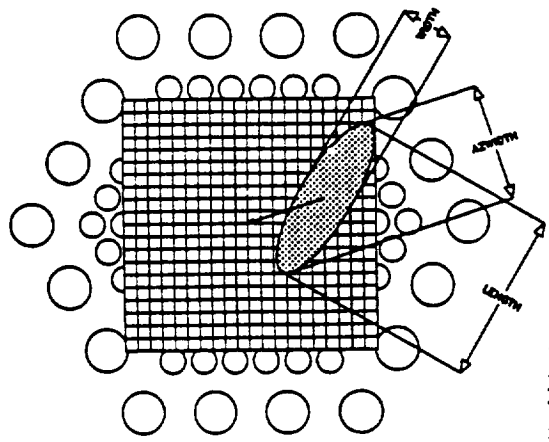

Figure 1.

Figure 1: A schematic diagram of the position analysis.
Figure 2: Histograms of data from the Crab Nebula: (a) ON; (b) OFF; (c) ON - OFF.
Figure 3: Contour plot of events from the 0.4° off-axis observations of the Crab Nebula.
Figure 4: A plot of X-ray and radio sources near Geminga. Large dotted circle: probable error for the location of Geminga. Shaded annulus: the 5-10 arc minute resolution predicted for EGRET. Inner radius of this ring corresponds to the measured resolution of the 10-meter Whipple telescope. Small circle: the one arc minute error obtainable with the Whipple twin Cherenkov air shower telescopes.

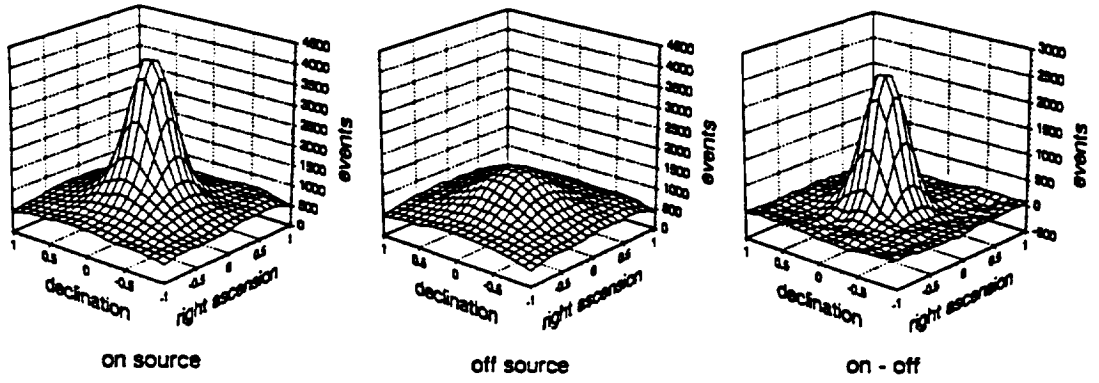

Figure 2.

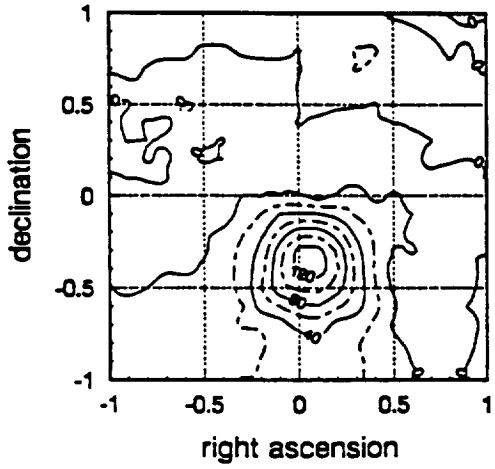

Figure 3.

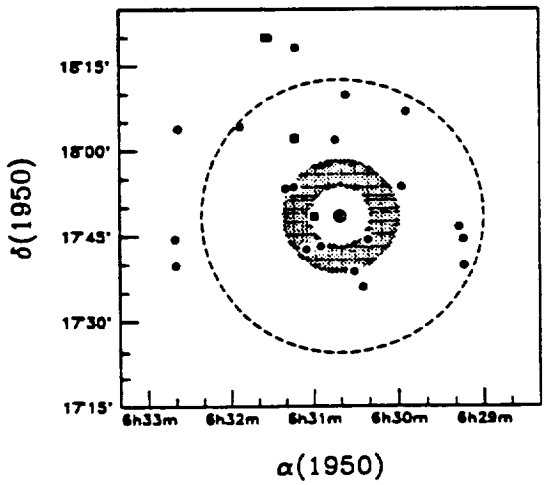

Figure 4.

ENERGY SPECTRUM DETERMINATION WITH THE ATMOSPHERIC CHERENKOV IMAGING TECHNIQUE

D.A. Lewis,[1] R.C. Lamb,[1] M.J. Lang,[2] D. Macomb,[3]
G. Mohanty,[1] T.C. Weekes,[4] and T. Whitaker[4]

[1] *Physics and Astronomy Department*
Iowa State University, Ames, IA 50011 USA
[2] *Physics Department, University College Dublin, Dublin 4, Ireland*
[3] *Computer Sciences Corp., GRO, NASA-Goddard, Greenbelt MD 20771 USA*
[4] *Whipple Observatory, P.O. Box 97, Amado, Arizona 85645 USA*

Abstract. Methods for determining the spectra of cosmic sources of Very High Energy gamma-radiation in the context of the atmospheric Cherenkov imaging technique are presented. Possible systematic biases in the extracted spectrum due to energy dependence in triggering, image selection and non-linearities in Cherenkov light vs. primary energy are discussed.

Introduction. Energy spectra of cosmic sources of TeV gamma-radiation are of primary importance in constraining possible acceleration mechanisms and in assessing source contributions to cosmic-ray fluxes. The atmospheric Cherenkov imaging technique[1] can significantly enrich the percentage of gamma-ray events relative to cosmic-ray background thus improving both the sensitivity of the instrument and also the accuracy with which the flux and spectrum of a source can be determined.

This paper is a progress report on methods being developed to determine source spectra with the Whipple Observatory Gamma-ray Telescope. Key steps are determination of the telescope collection area as a function of primary radiation energy and the telescope energy resolution function. The methods are based on extensive Monte Carlo simulations[2] at fixed primary photon energies and impact parameters relative to the telescope. In this paper basic ideas are presented; a complete re-analysis of the Crab spectrum will follow in a later publication.

Collection Area. The collection area of a telescope strongly depends on the energy of the incident radiation and the triggering mode of the telescope.[3] (The Whipple Observatory telescope normally is triggered when two or more photomultiplier tubes simultaneously detect more than a threshold number of photons[1].) In addition, if image shapes are also used to select gamma-ray-like events, the collection area also depends on the selection criteria. The collection area can be determined from Monte Carlo simulations as follows.

Let $N_{i,j}$ be the number of Monte Carlo showers launched with primary energy E_i at distance r_j from the location of the detector. The number of these showers that trigger the telescope *and* pass the gamma-ray selection criteria is given by $n_{i,j}$. In the limit of a large number of simulations, the trigger/pass-cut probability, $t_{i,j}$ is simply:

$$t(E_i, r_j) \cong n_{i,j}/N_{i,j}.$$

The collection area, $A(E_i)$ can then be written as

$$A(E_i) = \int_0^\infty t(E_i, r)\, 2\pi r\, dr \cong \sum_{r_j} t(E_i, r_j) \Delta A_j$$

where ΔA_j is the area associated with a ring centered at r_j.

In general, as the incident energy rises, the telescope trigger probability rises as well. Thus one might expect $t(E_i, r_j)$ to rise, flatten and asymtotically approach one as E_i increases. However, higher energy gamma-rays also tend to produce larger focal plane images as illustrated in Figure 1 which shows scatterplots of the Hillas[4] parameters *width* and *length* vs. shower energy at an impact parameter of 100 meters. The detector is assumed to be free of aberrations, noise and have perfect focal plane resolution with an infinite field of view for these simulations. The photomultiplier quantum efficiency is assumed to be 0.20.

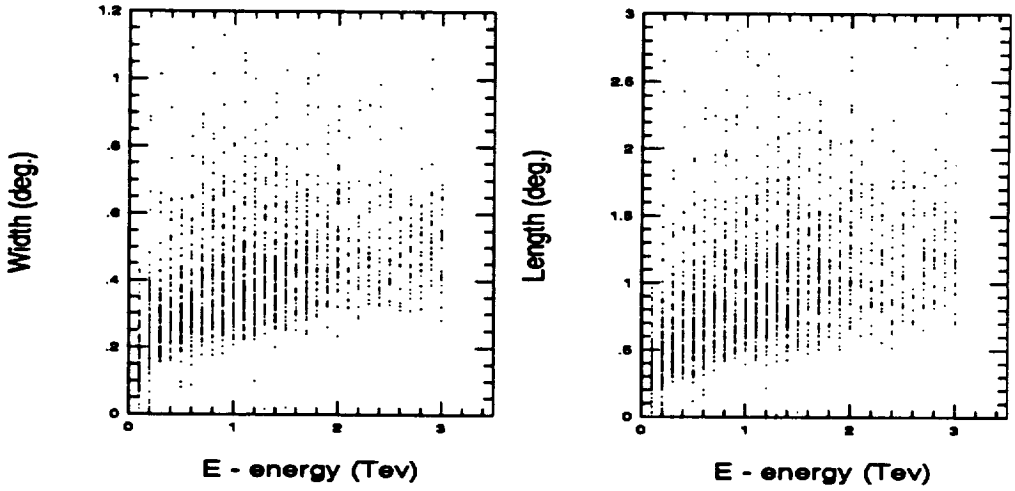

Figure 1. Correlation of shower image width and length with incident photon energy at $r = 100\,m$.

If gamma-ray selection criteria are chosen to be independent of estimated energy, then the collection area can fall with increasing energy because of the growth of shower image size. This, if uncorrected, can seriously distort the spectrum.

Energy Estimates and Resolution. As the energy increases, the total number number of detected photons, n_p, also increases, approximately linearly. Also, as the shower impact parameter (core-detector distance) increases the focal plane image moves out from optic axis. (Following Hillas[4] we call *dis* the angular distance from the optic axis to the centroid of the image.) The correlation of n_p with E at $r = 100\,m$ and of *dis* with r at $E = 0.6\,\mathrm{TeV}$ is shown in Figure 2 for the ideal detector described in the last section. As suggested by Plyasheshnikov and Konopelko,[5] the shower energy can be estimated as $\tilde{E} = f(n_p, dis)$. The dependence on *dis* should be relatively weak and the dependence on n_p is approximately linear.

For a given energy estimation function, $\tilde{E} = f(n_p, dis)$, the energy resolution function of the detector can be obtained from Monte Carlos as follows. Consider

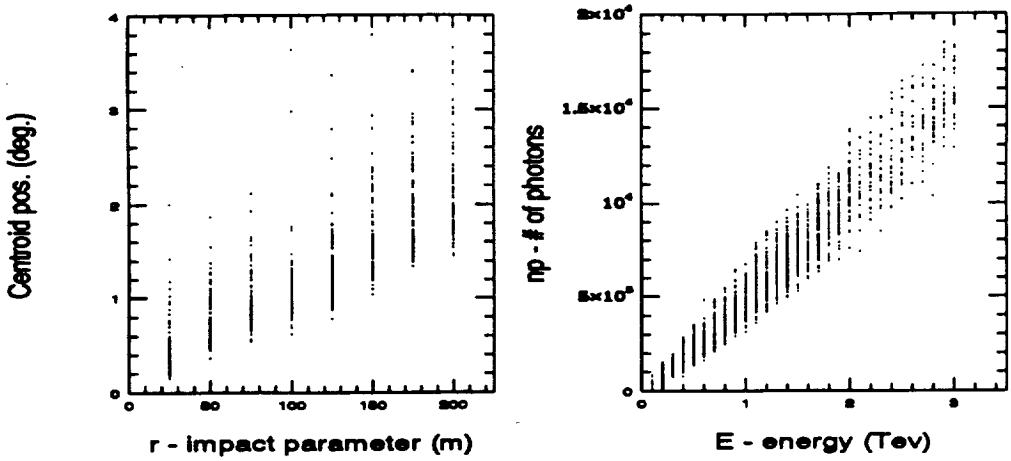

Figure 2. The correlations of centroid distance (dis) with impact parameter (r) and total light (n_p) with E at $r = 100\,m$ at $E = 0.6\,\mathrm{TeV}$ are shown above.

a set of simulations of N_{ij} showers with primary energy E_i at impact parameter r_j with n_{ij} of these triggering and passing the image cuts. The estimated energies for these n_{ij} simulated events are given by $\tilde{E}_{ij}^k$. The resolution function can then be written as shown below.

$$\psi(E_i, \tilde{E}) = \frac{1}{A(E_i)} \sum_j \{ \frac{\Delta A_j}{N_{ij}} \sum_{k=1}^{n_{ij}} \delta(\tilde{E} - \tilde{E}_{ij}^k) \}$$

The probability that primary energy E_i will appear in an estimated-energy interval $(\tilde{E}_k - \Delta\tilde{E}/2, \tilde{E}_k + \Delta\tilde{E}/2)$ is

$$\int_{\tilde{E}_k - \Delta\tilde{E}/2}^{\tilde{E}_k + \Delta\tilde{E}/2} \psi(E_i, \tilde{\alpha}) d\tilde{\alpha} = \frac{1}{A(E_i)} \sum_j \{ \frac{\Delta A_j}{N_{ij}} n_{ij}(\tilde{E}_k) \}$$

where $n_{ij}(\tilde{E}_k)$ is the number of Monte Carlo events at primary energy E_i and impact parameter r_j which trigger, pass the cuts, and have an estimated energy in the bin centered on $\tilde{E}_k$. Histogram versions of the resolution function can be obtained by integrating ψ over an appropriate bin size.

In order to minimize possible distortion of the extracted spectrum, the energy estimator $f(n_p, dis)$ should have essentially no bias, i.e., $\langle \tilde{E} \rangle$ must be equal to E_i for each of the Monte Carlo incident energies E_i where $\langle \tilde{E} \rangle$ is the average estimated energy from the Monte Carlos. It is given by:

$$\langle \tilde{E} \rangle = \int_0^\infty \psi(E_i, \tilde{E})\, \tilde{E}\, d\tilde{E} \cong \frac{1}{A(E_i)} \sum_j \{ \frac{\Delta A_j}{N_{ij}} \sum_{k=1}^{n_{ij}} \tilde{E}_{ij}^k \}$$

and the standard deviation can be found similarly.

Spectrum Determination. In a typical detection there is a set of events from the direction of the source and a similar set from an appropriately offset

background region of the sky. In order to make the discussion concrete, we will assume the "exposure" times are the same for both "on-source" and "off-source" regions. After selection criteria have been used to select gamma-ray-like events, an energy can be associated with each event under the assumption that it was caused by a primary gamma-ray. Assume that the results are binned in units of $\Delta\tilde{E}$ yielding histograms $n_{on}(\tilde{E}_k)$ and $n_{off}(\tilde{E}_k)$ for the on-source region and off-source regions respectively. The estimated number of gamma-ray events in each energy bin is then

$$\tilde{n}_\gamma(\tilde{E}_k) = n_{on}(\tilde{E}_k) - n_{off}(\tilde{E}_k)$$

and an estimate for the flux density at each energy is $\tilde{n}_\gamma(\tilde{E}_k)/\{A(\tilde{E}_k) \cdot \Delta\tilde{E} \cdot T\}$ where T is the length of the on-source observation.

If it is assumed that the differential spectrum is of the form βE^γ (rate/(area-energy)), and the Monte Carlos have a sufficient number of events so that their relative statistical error is small compared with the data, then β and γ can be found by minimizing the following.

$$\chi^2 = \sum_k \frac{\{\tilde{n}_\gamma(\tilde{E}_k) - \sum_i \beta T E_i^\gamma \Delta E \sum_j \Delta A_j \frac{n_{ij}(\tilde{E}_k)}{N_{ij}}\}^2}{n_{on}(\tilde{E}_k) + n_{off}(\tilde{E}_k)}$$

Note that χ^2 should be distributed with degrees of freedom equal to the number of energy bins minus two. The statistical errors in β and γ can also be estimated from the above.

It is also possible to estimate β and γ from integral spectra using the maximum likelihood method; other approaches have been discussed elsewhere[5,6].

Concluding Remarks. The questions of source *existence* and *energy spectrum* are quite distinct. Since fluxes generally fall rapidly with increasing energy, selection criteria optimized for source detection usually weight the low energy part of the spectrum more heavily. As the gamma-ray shower energy increases, the images tend to become larger and therefore more proton-like and may be preferentially rejected by selection criteria making it more difficult to make an accurate spectrum determination. The question of whether it is better to relax the cuts for higher energy events, or include the effect via the dependence of collection area on energy is currently being investigated.

References.

1. See paper by P.T. Reynolds, et al., in these proceedings.
2. The program used was originally written by T. Stanev using Unicas routines and has been extensively revised by G. Sembroski and D. Macomb. A description of the Unicas routines is in Stanev and Vankov, *Comp. Phys. Comm.* **16**, 363 (1979).
3. T.C. Weekes, Nuovo Cimento **32B**, 95 (1976).
4. A.M. Hillas, *Proc. 19th Internat. Cosmic Ray Conf.*, (La Jolla), **3**, 445 (1985).
5. A.V. Plyasheshnikov and A.K. Konopelko, (1989) Proc. Intl. Workshop on VHE Gamma-Ray Astronomy, p. 115 and p. 120.
6. G. Vacanti et al., (1991) to be published in Ap. J.; see also the paper in these proceedings.